

Dielectric, Electrical Conductivity Behavior and Molecular Modeling of Some Pyrimidine and Purine Compounds

MS Masoud^{1*}, M Sh Ramadan¹, AM Sweyllam² and MH Al-Saify³

¹Chemistry Department, Faculty of Science, Alexandria University, Alexandria, Egypt

²Physics Department, Faculty of Science, Alexandria University, Alexandria, Egypt

³Sidi Kerir Petrochemicals Company, Alexandria, Egypt

*Corresponding author

MS Masoud, Chemistry Department, Faculty of Science, Alexandria University, Alexandria, Egypt

Submitted: 02 Apr 2021; Accepted: 09 Apr 2021; Published: 27 Apr 2021

Citation: MS Masoud, M Sh Ramadan, AM Sweyllam and MH Al-Saify (2021) Dielectric, Electrical Conductivity Behavior and Molecular Modeling of Some Pyrimidine and Purine Compounds. *J Chem Edu Res Prac* 5: 64-88.

Abstract

The dielectric and electrical conductivity measurements for biologically active nucleic acid compounds reveal semiconducting properties and small relaxation times. On the basis of electronic transition within molecules, two pathways for the conduction of electricity may be expected. The first conducting process occurring in the lower temperature region is attributed to $n \rightarrow \pi^*$ transitions which require less energy to be performed. In the upper temperature region, conduction could be attributed to $\pi \rightarrow \pi^*$ transitions which need more energy to participate in electronic conduction. The observed increment of conduction in the upper temperature region may be attributed to interactions between $n \rightarrow \pi^*$ and $\pi \rightarrow \pi^*$ transitions. Quantum chemical parameters such as the highest occupied molecular orbital energy (E_{HOMO}) and the lowest unoccupied molecular orbital energy (E_{LUMO}) were given using molecular modeling. Energy gap (ΔE) and parameters which give information about the reactive chemical behavior of compounds such as electronegativity (χ), chemical potential (μ), global hardness (η), softness (σ) and electrophilicity index (ω) were calculated.

Keywords: Dielectric, Electrical Conductivity, Capacitance (Cp), Loss Tangent ($\tan \delta$), Cole-Cole Diagram, Relaxation Time (τ), Activation Energy, Molecular Modeling

Introduction

Dielectric measurements are important methods for studying the dynamic properties (capacitance, impedance, permittivity and loss factor) of dielectrics. This behavior was associated with a hopping mechanism in terms of correlated barrier hopping (CBH) model for alternating current (a.c.) loss, first developed by Pike for single-electron hopping, and has been extended by Elliot for simultaneous two electrons hopping [1, 2].

The dielectric relaxation studies are important to understand the nature and the origin of dielectric losses, which in turn, may be useful in the determination of the structure and defects in solids [3-7].

In recent years, the study of the electrical conduction mechanism in organic compounds has been the subject of many theoretical and experimental investigations. The interest of this topic is stimulated by the applications of these compounds in the development of various modern and future technologies of solid-state devices. Moreover, the information about the electrical properties of mate-

rials is also necessary for determining the optimum conditions and analysis of electrical transport in these materials. Also, both direct current (d.c.) and alternating current (a.c.) measurements provide important information about the conduction process and the predominant charge transport mechanism within an organic material [7].

Organic semiconductors are of steadily growing interest as active components in electronics and opto-electronics. Due to their flexibility, low cost and ease of production they represent a valid alternative to conventional inorganic semiconductor technology [8].

The increasing environmental consciousness throughout the world has triggered a search for new products and processes that are compatible with the environment.

Experimental

Synthesis of Metal Complexes in The Solid State

These were prepared by mixing metal chloride solutions with li-

gand solutions, Table (1), hence they were refluxed, filtered and dried for the separated products. The metal ions were determined by atomic absorption techniques and complexometric titrations using published procedures [9]. The complexes were digested by aqua regia several times to complete decomposition for the organic ligand compounds. The analyzed complexes were given in Table (2a-b).

Instruments and Working Procedures

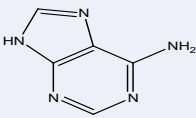
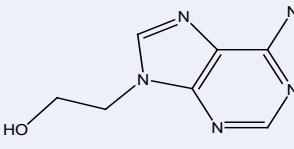
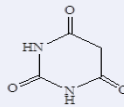
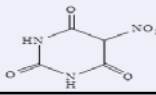
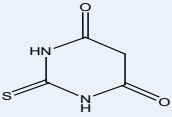
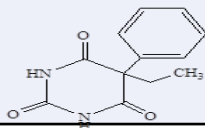
Dielectric and Electrical Conductivity Measurements

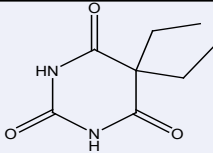
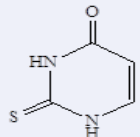
- Four test parameters including impedance $|Z|$, phase angle θ , parallel equivalent static capacitance C_p and loss tangent $\tan \delta$ were measured for the ligands and complexes in the solid state at constant voltage 0.80 volt but different temperatures (40-240°C) and at variable frequencies (500 Hz - 5 MHz) using HIOKI "3532-50 LCR HITESTER" instrument.
- The ligands and complexes were prepared in the form of tablets at a pressure of 6-7 tons/cm² with 10 mm diameter and 0.7-4.4 mm thickness. Silver metal was evaporized on the major faces of each test piece to improve the contact with the measuring electrodes. The tablets were hold between two copper electrodes and then inserted with the holder vertically into cylindrical electric furnace. The potential drop across the heater was varied gradually through variable transformer to produce slow rate of increasing the temperature to get accurate temperature measurements using a pre-calibrated Cu-constantan thermocouple attached to the sample.
- The dielectric constant ϵ , the dielectric loss ϵ'' , real part of impedance Z' , imaginary part Z'' , the conductivities $\sigma_{a.c.}$ (a.c.: alternating current condition), the relaxation times τ_0 , τ and the activation energies ΔE of the ligands and complexes were calculated [10].

Molecular Modeling

The ChemOffice Ultra 2004 computer and HyberChem programs are used for molecular modeling studies of the ligands and their complexes.

Table 1: Names, abbreviations, m.p. and structures of the ligands are given*.

| Compound | Abbreviation | M.P.°C | Structures |
|------------------------|--------------|---------|---|
| Adenine | (AD) | 360-365 |  |
| 9-Hydroxyethyladenine | (HEAD) | 244 |  |
| Barbituric acid | (BA) | 248 |  |
| 5-Nitrobarbituric acid | (NBA) | 176 |  |
| Thiobarbituric acid | (TBA) | 245 |  |
| Phenobarbital | (PB) | 174-178 |  |

| | | | |
|--------------|------|-----|--|
| Barbital | (B) | 190 |  |
| 2-Thiouracil | (TU) | 340 |  |

Cont.

* All these ligands are of white colour except TBA is of yellow colour and were purchased from BDH company.

Table 2a: C, H, N, S elemental analysis for some nucleic acid constituent complexes.

| Complex | Colour | Formula | Calculated/(Found) % | | | |
|---|--------|---|----------------------|--------|---------|---------|
| | | | C | H | N | S |
| Co-Ni(TU) ₃ ·4H ₂ O | brown | C ₁₂ H ₁₆ N ₆ O ₇ S ₃ CoNi | 25.28 | 2.83 | 14.74 | 16.87 |
| | | | (25.00) | (2.80) | (15.20) | (17.00) |
| Hg(BA) ₂ | buff | C ₈ H ₆ N ₄ O ₆ Hg | 21.13 | 1.33 | 12.32 | - |
| | | | (21.60) | (1.52) | (12.51) | (-) |

Table 2b: H, N, S, M elemental analysis for some nucleic acid constituent complexes.

| Complex | Colour | Formula | Calculated/(Found) % | | | |
|---|--------|---|----------------------|---------|---------|---------|
| | | | H | N | S | M |
| Cr(TU)(OH) ₂ ·H ₂ O | green | C ₄ H ₇ N ₂ O ₄ SCr | 3.05 | 12.12 | 13.87 | 22.49 |
| | | | (3.32) | (12.50) | (14.00) | (22.66) |
| Mn(TU) ₂ ·H ₂ O | brown | C ₁₆ H ₁₆ N ₈ O ₅ S ₄ Mn | 2.76 | 19.21 | 21.98 | 9.41 |
| | | | (3.00) | (20.00) | (22.00) | (9.88) |
| Hg(TU) ₂ ·4H ₂ O | white | C ₈ H ₁₄ N ₄ O ₆ S ₂ Hg | 2.68 | 10.63 | 12.17 | 38.07 |
| | | | (3.00) | (11.00) | (12.00) | (38.12) |

Results and Discussion

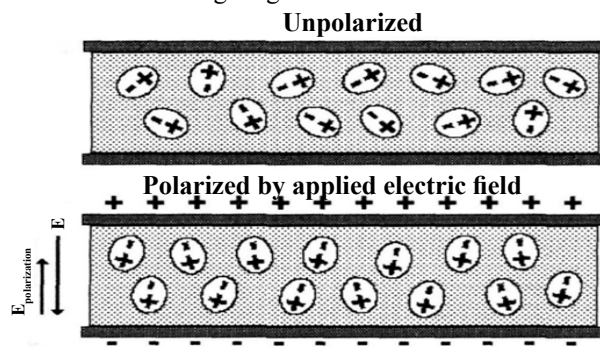
Dielectric and Electrical Conductivity Measurements

Dielectric Measurements

A dielectric materials measurement can provide critical design parameter information for many electronics applications. For example, the loss of a cable insulator, the impedance of a substrate, or the frequency of a dielectric resonator can be related to its dielectric properties. The information is also useful for improving ferrite, absorber, and packaging designs. More recent applications in the area of industrial microwave processing of food, rubber, plastic and ceramics have also been found to benefit from knowledge of dielectric properties.

The dielectric behaviors of materials under external (a.c.) field have high scientific and technological importances. In polar dielectrics, the molecules, which are normally composed of two or more different atoms, have dipole moments even in the absence of an electric field, that is, the centres of their positive and negative charges do not coincide [11]. Normally the molecular dipoles are

randomly oriented throughout the material owing to thermal agitation, so that the average moment over any macroscopic volume element is zero. In the presence of an externally applied field, the molecules tend to orient themselves in the direction of the field as shown in the following diagram:



For a parallel-plate condenser in which a dielectric tablet fills the

space between the plates, the capacitance is given by [12]:

$$C_p = A\epsilon\epsilon_0 / d$$

Where ϵ_0 is the permittivity of a vacuum and its value is approximately $8.854 \times 10^{-12} \text{ F m}^{-1}$, ϵ is the dielectric constant of a dielectric, A and d are the area and the thickness of the matter tablet, respectively.

The complex dielectric permittivity, $\epsilon^*(\omega)$ is given as follows [13]:

$$\epsilon^*(\omega) = \epsilon'(\omega) - i\epsilon''(\omega)$$

where $\epsilon'(\omega)$ and $\epsilon''(\omega)$ are the real and imaginary parts of the complex permittivity, respectively. ω is the angular frequency, $\omega = 2\pi f$ and $i = \sqrt{-1}$.

$$\epsilon'(\omega) = \epsilon \sin \theta, \epsilon''(\omega) = \epsilon \cos \theta$$

where θ is the phase shift.

$$\text{The loss tangent, } \tan \delta = \epsilon''/\epsilon', \delta = 90^\circ - \theta$$

The real and imaginary parts of the complex impedance are given by:

$$Z' = Z \cos \theta, Z'' = Z \sin \theta$$

where Z' and Z'' are the real and imaginary parts of the impedance, respectively.

Dispersion arising during the transition from full orientational polarization at zero or low frequencies to negligible orientational polarization at high radio frequencies is referred to as dielectric relaxation [14].

The rate of decay and build-up of the orientational polarization, as given by the relaxation time τ , will depend upon the thermal energy of the dipoles as well as upon the internal or molecular friction forces encountered by the rotating dipoles.

The dielectric parameters for the investigated ligands and complexes are illustrated in terms of temperature and frequency ($\ln f$) changes, Figures (1-12). The more spotlight points, could be given as follows:

1. The capacitance (C_p) decreases with increasing the applied frequency in some different ranges which may be attributed to the effect of charge redistribution by carrier hopping on defects [15, 16]. At low frequency, the charge on defects can be rapidly redistributed so that defects closer to the positive side of the applied field become negatively charged, while defects closer to the negative side of the applied field become positively charged. This leads to screening of the field and an overall reduction in the electric field. Because capacitance is inversely proportional to the field, this reduction in the field for a given voltage results in the increased capacitance observed as the frequency is lowered. In case of high frequency, the defects no longer have enough time to rearrange in response to the applied voltage, hence the capacitance decreases.
2. ϵ' and ϵ'' decrease with increasing frequency ($\ln f$), which can be explained as follows:
 - (a) At low frequencies the dielectric constant for polar materials is due to the contribution of multi-component of polarizability, deformational polarization (electronic and ionic polarization) and relaxation polarization (orientational and interfacial polarization) [17].

(b) When the frequency begins to increase, the dipoles will no longer be able to rotate sufficiently rapidly, so that their oscillations begin to lag behind those of the field. As the frequency is further increased, the dipole will be completely unable to follow the field and the orientation polarization stopped, so ϵ' and ϵ'' decrease at higher frequencies approaching a constant value due to the interfacial or space charge polarization only [4, 18].

3. The relative permittivity and dielectric loss values for the complexes, Figures (8-12), reveal semiconducting features based mainly on the hopping mechanism [19].
4. The loss tangent ($\tan \delta$) is decreased with increasing frequency, while at certain temperatures for ligands (HEAD, NBA) and complexes ($\text{Cr(TU)(OH)}_2 \cdot \text{H}_2\text{O}$, $\text{Mn(TU)}_2 \cdot \text{H}_2\text{O}$, $\text{Co-Ni(TU)}_3 \cdot 4\text{H}_2\text{O}$, $\text{Hg(TU)}_2 \cdot 4\text{H}_2\text{O}$) a well-defined peaks are observed corresponding to dielectric relaxation phenomena, Figures (2, 4, 9-12) [20].
5. The impedance (Z) is mostly decreased with increasing frequency, Figures (1-12). The Z'' - Z' relationships are illustrated in Figures (13, 14) at different temperatures.

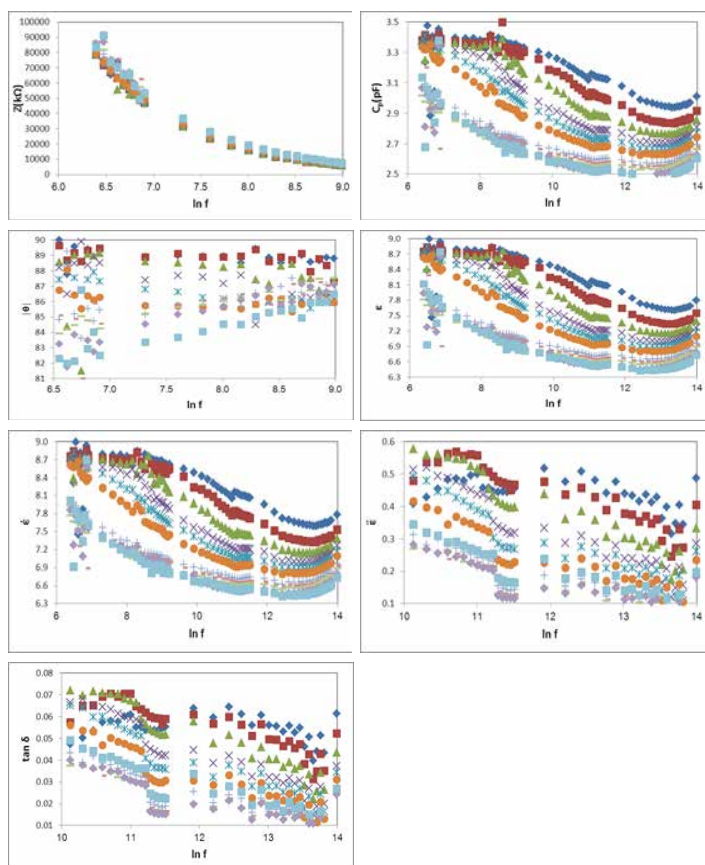


Figure 1: The dielectric parameters (Z , C_p , $|\theta|$, ϵ , ϵ' , ϵ'' , $\tan \delta$) - $\ln f$ relationships for AD at different temperatures $\blacklozenge 40^\circ\text{C}$, $\blacksquare 60^\circ\text{C}$, $\blacktriangle 80^\circ\text{C}$, $\times 100^\circ\text{C}$, $\bullet 120^\circ\text{C}$, $\blacklozenge 140^\circ\text{C}$, $\blacksquare 160^\circ\text{C}$, $\blacktriangle 180^\circ\text{C}$, $\times 200^\circ\text{C}$, $\bullet 220^\circ\text{C}$ and $\blacklozenge 240^\circ\text{C}$

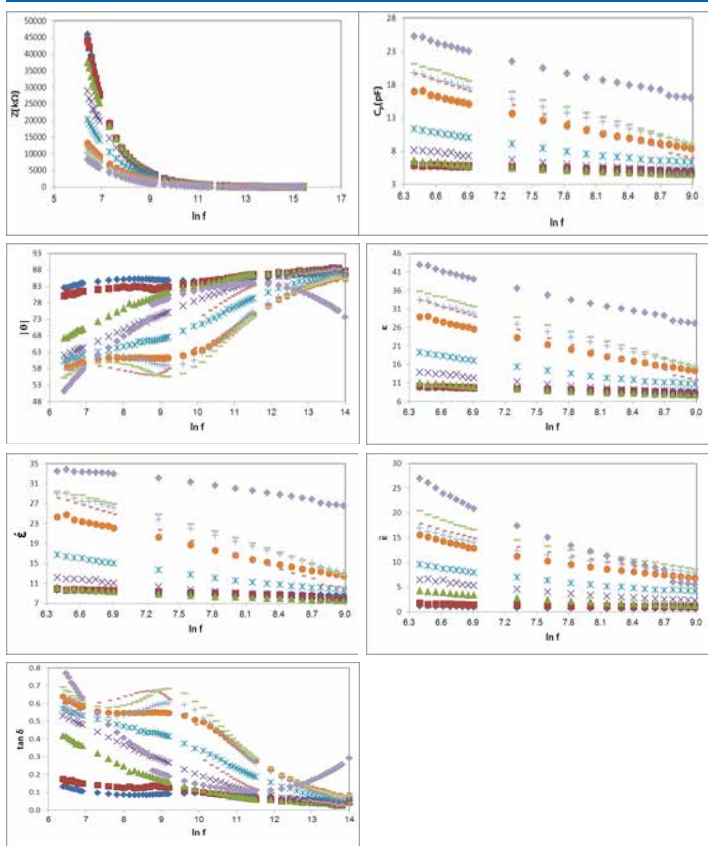


Figure 2: The dielectric parameters (Z , C_p , $|\theta|$, ϵ' , ϵ'' , $\tan \delta$) - $\ln f$ relationships for HEAD at different temperatures 40°C , 60°C , 80°C , 100°C , 120°C , 140°C , 160°C , 180°C , 200°C and 220°C

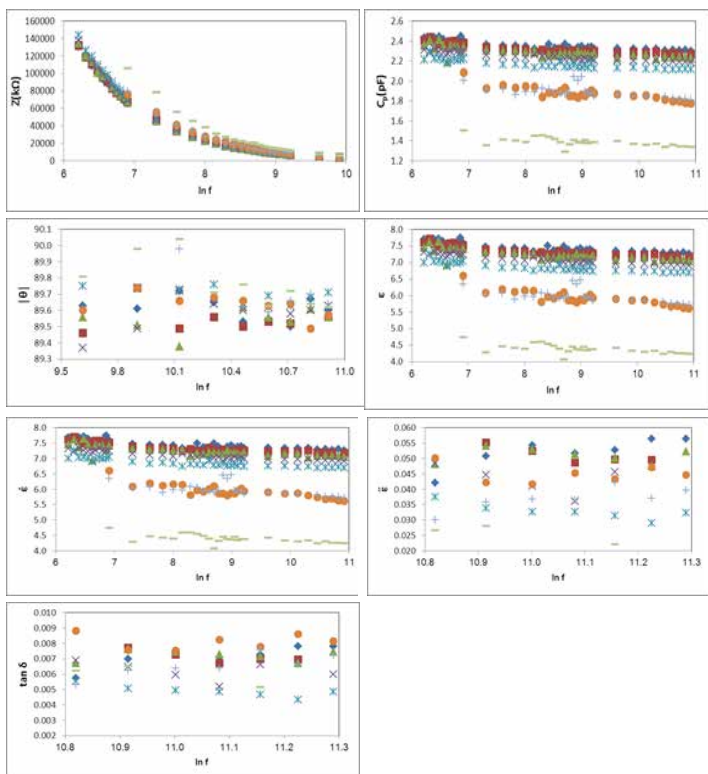


Figure 3: The dielectric parameters (Z , C_p , $|\theta|$, ϵ' , ϵ'' , $\tan \delta$) -

$\ln f$ relationships for TBA at different temperatures 40°C , 60°C , 80°C , 100°C , 120°C , 140°C , 160°C , 180°C and 200°C

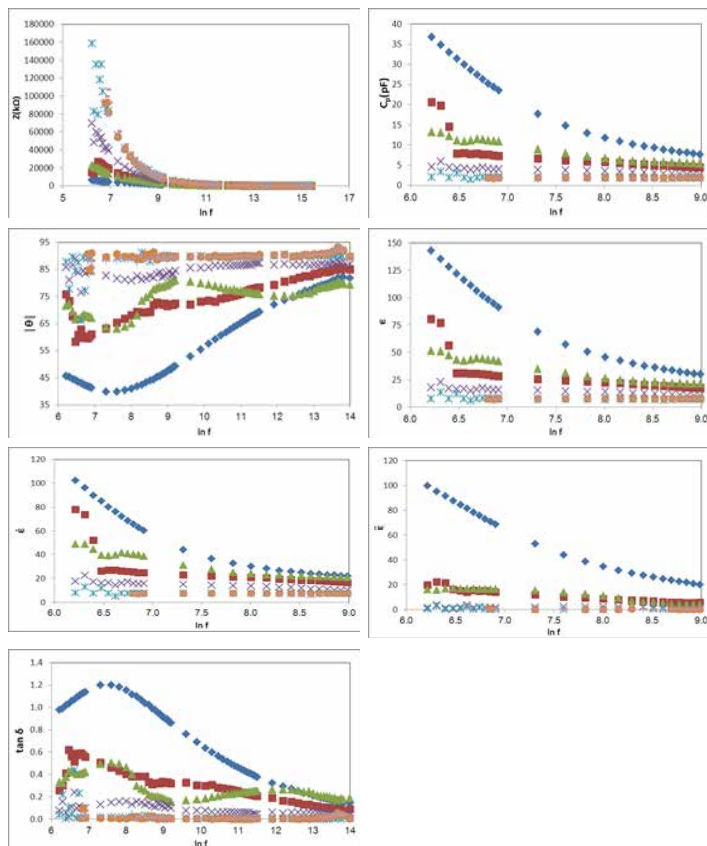
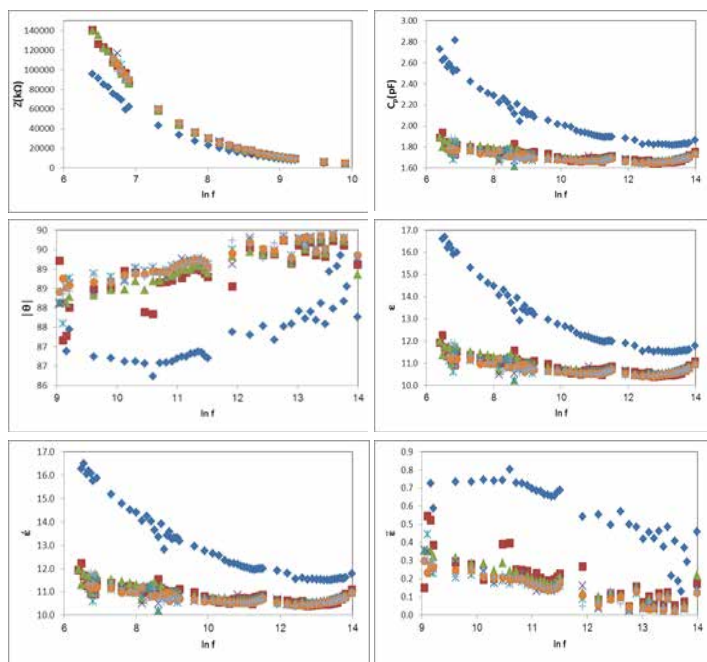


Figure 4: The dielectric parameters (Z , C_p , $|\theta|$, ϵ' , ϵ'' , $\tan \delta$) - $\ln f$ relationships for NBA at different temperatures 40°C , 60°C , 80°C , 100°C , 120°C , 140°C , 160°C and 170°C



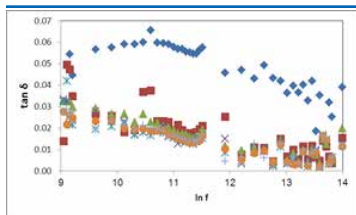


Figure 5: The dielectric parameters (Z , C_p , $|\theta|$, ϵ , ϵ' , ϵ'' , $\tan \delta$) - $\ln f$ relationships for B at different temperatures \blacklozenge 40°C, \blacksquare 60°C, \blacktriangle 80°C, \times 100°C, \times 120°C, \blacksquare 140°C and \blacklozenge 160°C

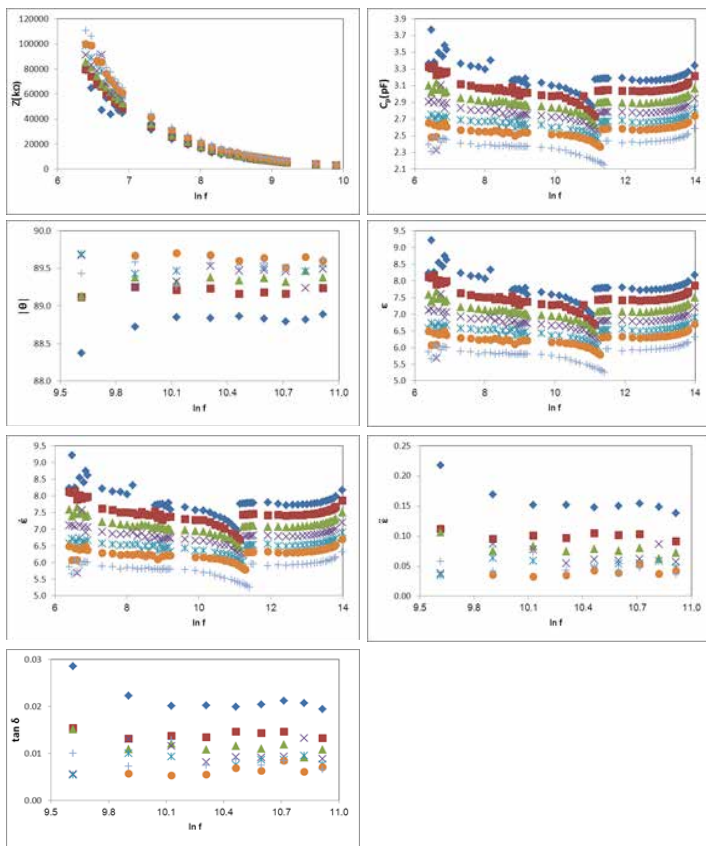


Figure 6: The dielectric parameters (Z , C_p , $|\theta|$, ϵ , ϵ' , ϵ'' , $\tan \delta$) - $\ln f$ relationships for PB at different temperatures \blacklozenge 40°C, \blacksquare 60°C, \blacktriangle 80°C, \times 100°C, \times 120°C, \blacksquare 140°C and \blacklozenge 150°C

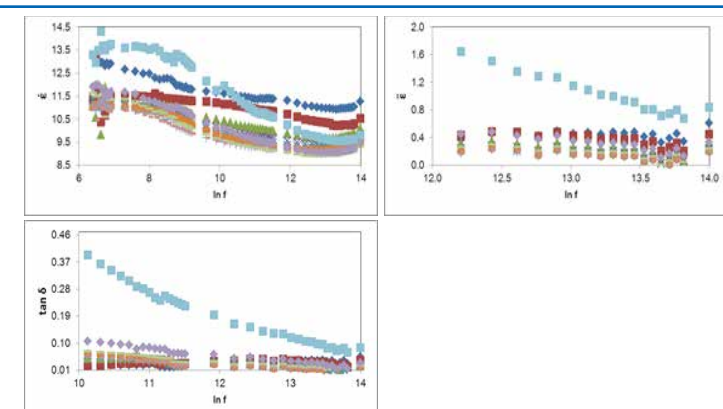
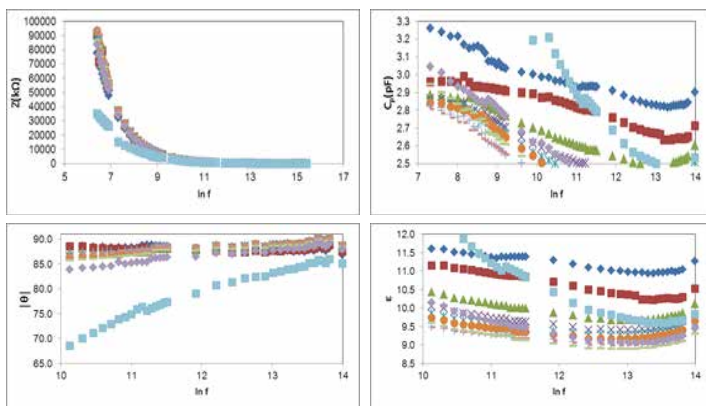


Figure 7: The dielectric parameters (Z , C_p , $|\theta|$, ϵ , ϵ' , ϵ'' , $\tan \delta$) - $\ln f$ relationships for TU at different temperatures \blacklozenge 40°C, \blacksquare 60°C, \blacktriangle 80°C, \times 100°C, \times 120°C, \blacksquare 140°C, \blacksquare 160°C, \blacksquare 180°C, \blacksquare 200°C, \blacklozenge 220°C and \blacklozenge 240°C

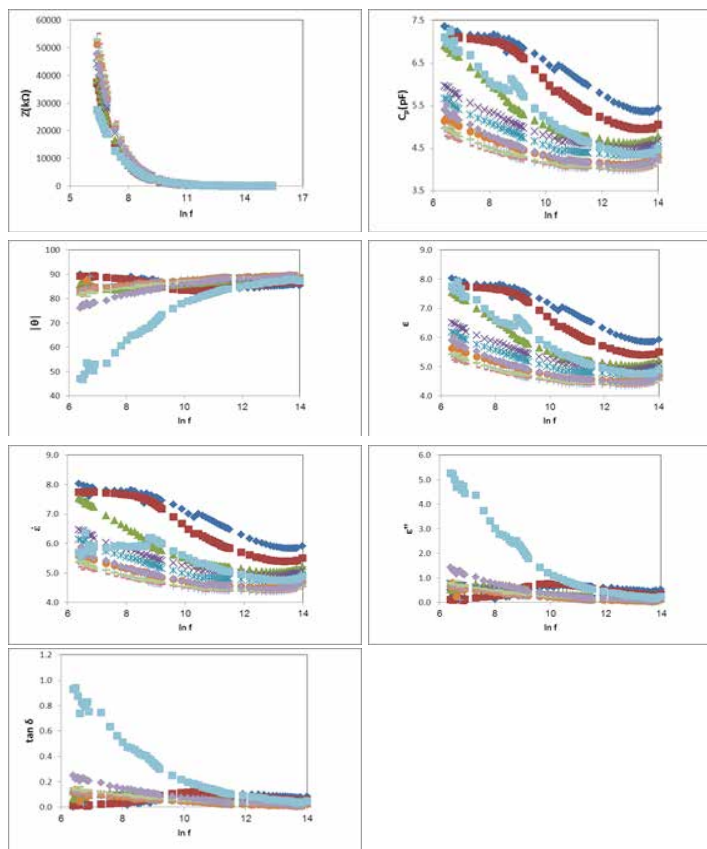


Figure 8: The dielectric parameters (Z , C_p , $|\theta|$, ϵ , ϵ' , ϵ'' , $\tan \delta$) - $\ln f$ relationships for $\text{Hg}(\text{BA})_2$ at different temperatures \blacklozenge 40°C, \blacksquare 60°C, \blacktriangle 80°C, \times 100°C, \times 120°C, \blacksquare 140°C, \blacksquare 160°C, \blacksquare 180°C, \blacksquare 200°C, \blacklozenge 220°C and \blacklozenge 240°C

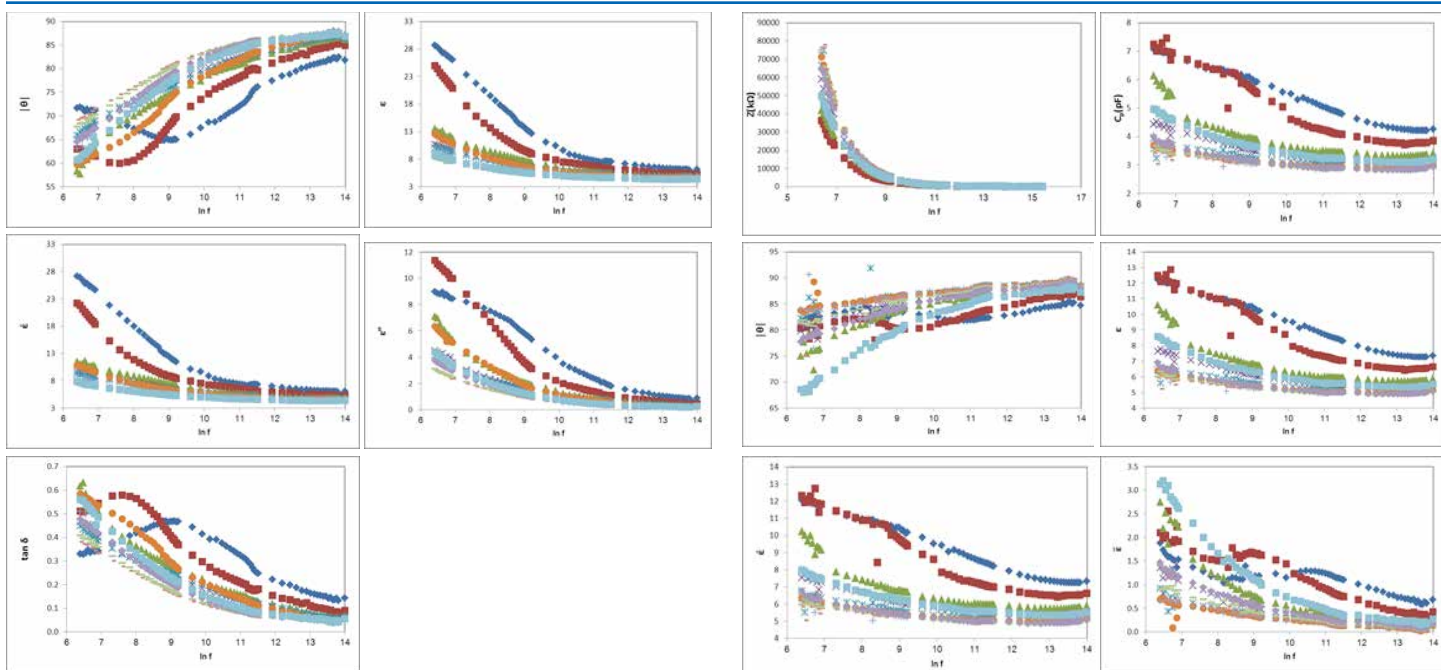


Figure 9: The dielectric parameters (Z , C_p , $|\theta|$, ϵ , ϵ' , ϵ'' , $\tan \delta$) - $\ln f$ relationships for $\text{Cr}(\text{TU})(\text{OH})_2 \cdot \text{H}_2\text{O}$ at different temperatures 40°C , 60°C , 80°C , 100°C , 120°C , 140°C , 160°C , 180°C , 200°C , 220°C and 240°C .

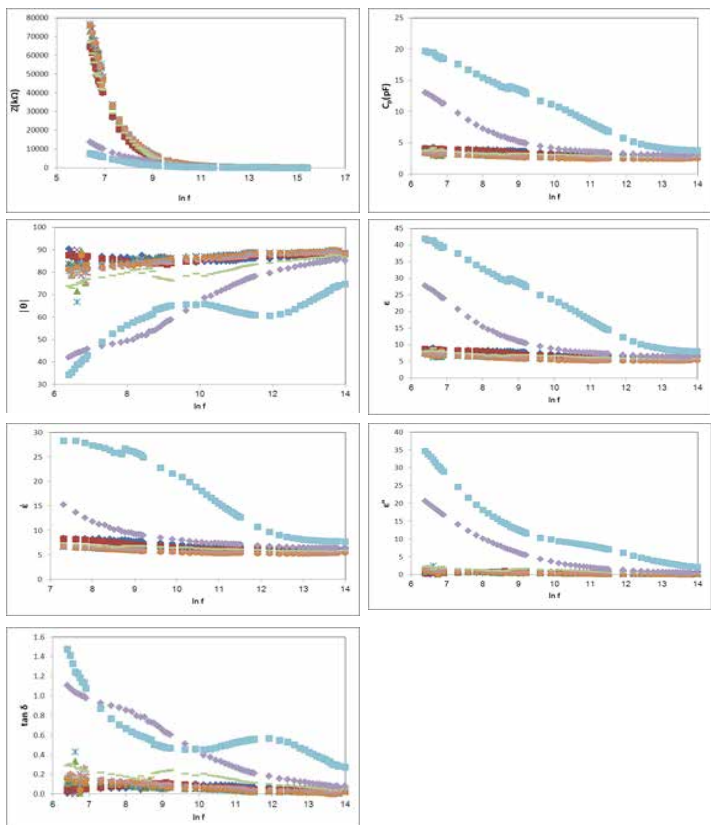


Figure 10: The dielectric parameters (Z , C_p , $|\theta|$, ϵ , ϵ' , ϵ'' , $\tan \delta$) - $\ln f$ relationships for $\text{Mn}(\text{TU})_2 \cdot \text{H}_2\text{O}$ at different temperatures 40°C , 60°C , 80°C , 100°C , 120°C , 140°C , 160°C , 180°C , 200°C , 220°C and 240°C .

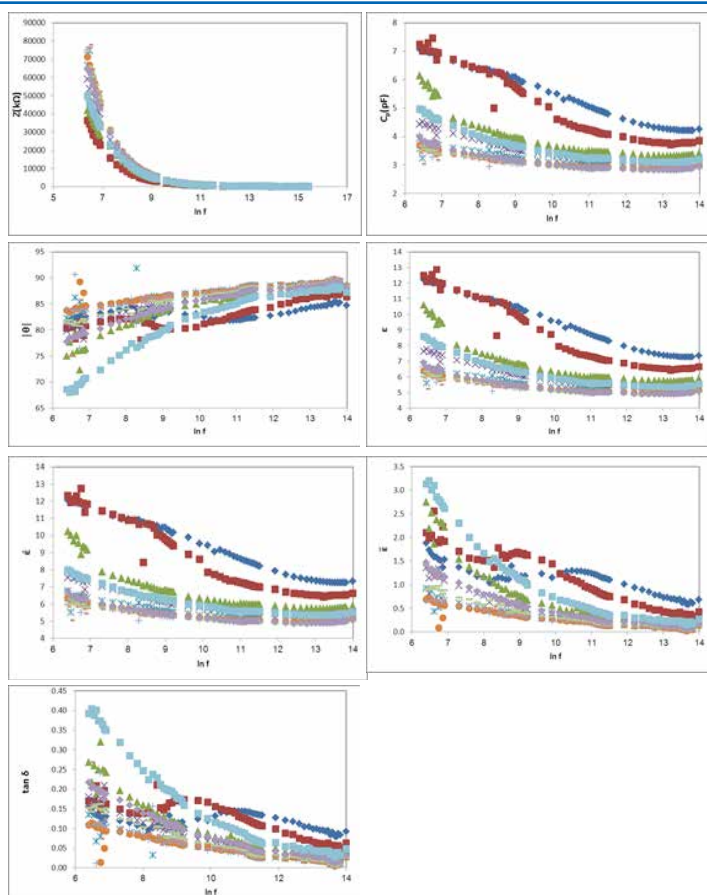
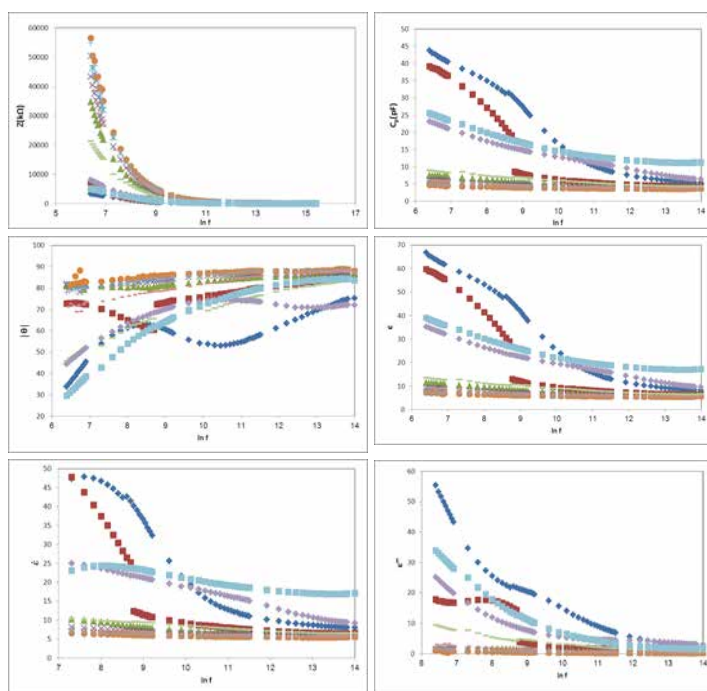


Figure 11: The dielectric parameters (Z , C_p , $|\theta|$, ϵ , ϵ' , ϵ'' , $\tan \delta$) - $\ln f$ relationships for $\text{Co-Ni}(\text{TU})_3 \cdot 4\text{H}_2\text{O}$ at different temperatures 40°C , 60°C , 80°C , 100°C , 120°C , 140°C , 160°C , 180°C , 200°C , 220°C and 240°C .



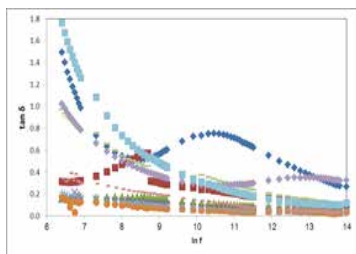


Figure 12: The dielectric parameters (Z , C_p , $|\theta|$, ϵ , ϵ' , ϵ'' , $\tan \delta$) - $\ln f$ relationships for $\text{Hg}(\text{TU})_2 \cdot 4\text{H}_2\text{O}$ at different temperatures $\blacklozenge 40^\circ\text{C}$, $\blacksquare 60^\circ\text{C}$, $\blacktriangle 80^\circ\text{C}$, $\times 100^\circ\text{C}$, $\star 120^\circ\text{C}$, $\blacklozenge 140^\circ\text{C}$, $\blacklozenge 160^\circ\text{C}$, $\blacklozenge 180^\circ\text{C}$, $\blacklozenge 200^\circ\text{C}$, $\blacklozenge 220^\circ\text{C}$ and $\blacksquare 240^\circ\text{C}$

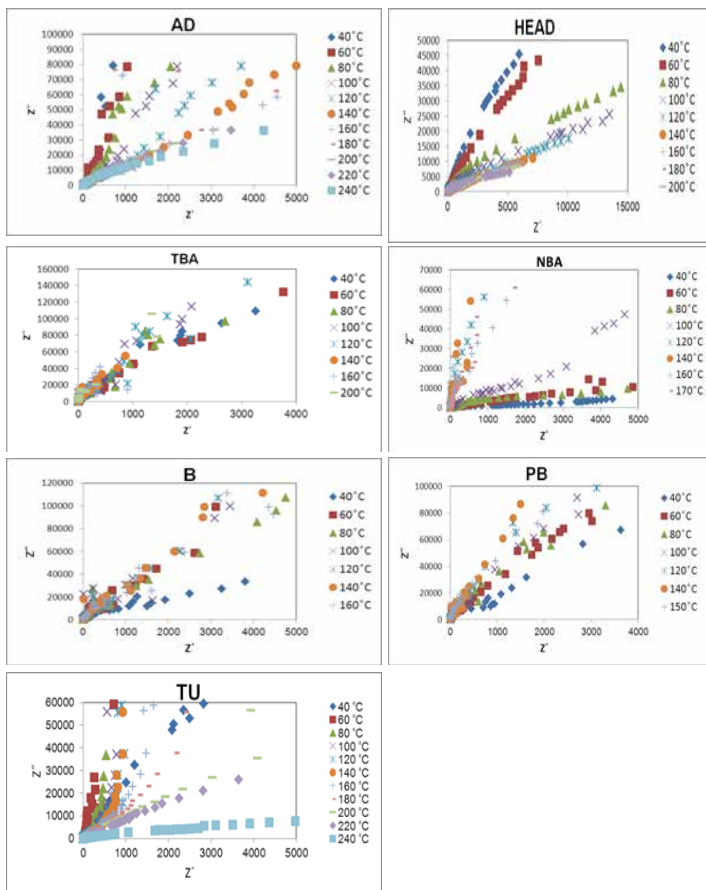


Figure 13: Z'' - Z' relationship for ligands at different temperatures

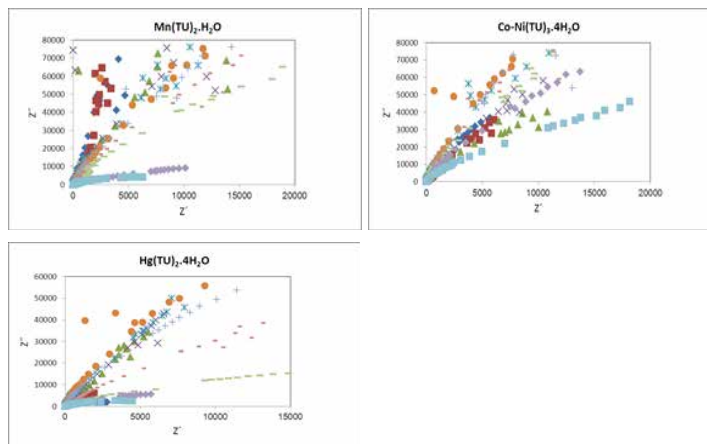
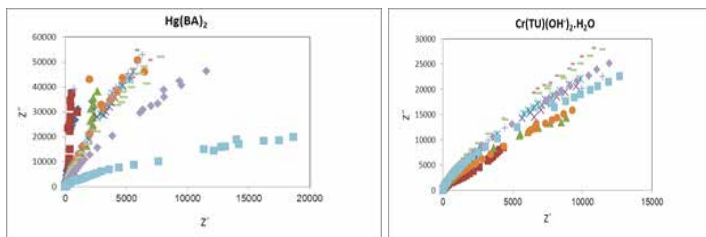


Figure 14: Z'' - Z' relationship for complexes at different temperatures $\blacklozenge 40^\circ\text{C}$, $\blacksquare 60^\circ\text{C}$, $\blacktriangle 80^\circ\text{C}$, $\times 100^\circ\text{C}$, $\star 120^\circ\text{C}$, $\blacklozenge 140^\circ\text{C}$, $\blacklozenge 160^\circ\text{C}$, $\blacklozenge 180^\circ\text{C}$, $\blacklozenge 200^\circ\text{C}$, and $\blacksquare 240^\circ\text{C}$

The evaluation of experimental dielectric data is much facilitated by certain graphical methods of display, which permit the derivation of parameters by geometrical construction. The earliest and most used of these methods consists of plotting the imaginary part $\epsilon''(\omega)$ for a certain frequency against the real part $\epsilon'(\omega)$ at the same frequency, in cartesian coordinates or in the complex plane [21]. This diagram may be called the complex locus diagram or Argand diagram and was applied to dielectrics by Cole and Cole, illustrated in a familiar plot or arc plot [22].

For a dielectric with a single relaxation time the Cole-Cole plot is a semi-circle which provides an elegant method of finding out whether a system has a single relaxation time or more. The arc plot of a dielectric with a single relaxation time is illustrated in Figure (15(a) and (b)).

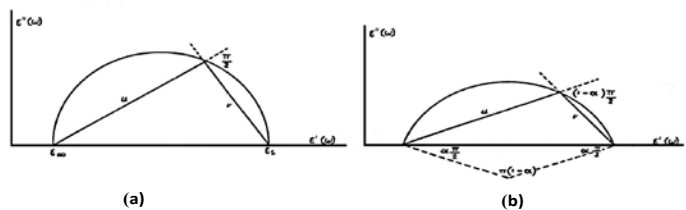


Figure 15: (a) Arc plot for a Debye dielectric; (b) Arc plot for a dielectric with a Cole-Cole distribution characterized by the parameter α (from Cole and Cole) [22].

For polar compounds, a semi-circle is obtained on plotting $\epsilon''(\omega)$ against $\epsilon'(\omega)$ for each temperature [23]. A given point on the semi-circle corresponds to a given frequency while the summit corresponds to $\omega\tau = 1$, Figure (15(a) and (b)). The plot has the disadvantage that ω does not appear in it. This semi-circle Cole-Cole diagram has been used to determine the distribution parameter α , which measures the width of distribution of relaxation time. Also, the macroscopic relaxation time τ_0 and the molecular relaxation time τ can be determined [17, 22]. α values are evaluated by mea-

suring the angle between the real part of dielectric constant and radius of the circle.

If the centres of semi-circles lie $\epsilon'(\omega)$ axis, α is zero (Debye type). Otherwise, the centre is below $\epsilon'(\omega)$ axis and $\alpha \neq 0$ (non-Debye type) [24]. Two intersections between the real axis $\epsilon'(\omega)$ and the circular arc, give the relative permittivity at zero frequency (static dielectric constant ϵ_s) and that at infinite frequency approaching the frequencies of light oscillators (optical dielectric constant ϵ_∞) [17]. A point on the semi-circle defines two vectors u and v , Figure (15 (a and b)), v is the distance on the Cole-Cole diagram between the static dielectric constant ϵ_s and the experimental point, u is the distance between that point and the optical dielectric constant ϵ_∞ . Cole and Cole generalized the representation of a Debye dielectric by a circular arc plot in the complex plane so that it is applied to a certain type of distributions of relaxation times, so

$$v/u = (\omega\tau_0)^{1-\alpha}$$

where ω is the angular frequency. The parameter α equals zero when the compound has only one relaxation time, whereas for a series of relaxation times, the value of α varies between 0 and 1. The extent of the distribution of relaxation times increases with increasing parameter α . On the other hand, the value of τ_0 decreases with increasing temperature [22]. The molecular relaxation time τ could be determined based on the following equation [22]:

$$\tau = \frac{2\epsilon_s + \epsilon_\infty}{3\epsilon_s} \tau_0$$

The relaxation time is interpreted as the average time which a molecule spends in one of the equilibrium positions before jumping to the other one. The temperature dependence of τ can be expressed for thermally activated processes as [17]:

$$\tau = \tau_0 e^{E_a/kT}$$

where τ_0 is a constant characteristic relaxation time and represents the time of a single oscillation of a dipole in a potential well, E_a is the energy of activation for the relaxation of the dipole, k is the Boltzmann constant and τ represents the average or most probable value of the spread of the relaxation times. The Cole-Cole diagrams for the investigated ligands and complexes at different temperatures, Figures (16-27), reveal mainly non-Debye type [24].

The dielectric data obtained from the analysis of Cole-Cole diagrams for different ligands and complexes are collected in Table (3).

One must focus the attention that the molecular orientation and the association in molecular structure are important.

The variation of $\ln \tau$ as a function of reciprocal absolute temperature for different ligands and complexes, Figures (28, 29), assigned that as the temperature increases, the relaxation time for each relaxator becomes smaller in some ranges.

The activation energies for the relaxation processes of different ligands and complexes are given in Table (4).

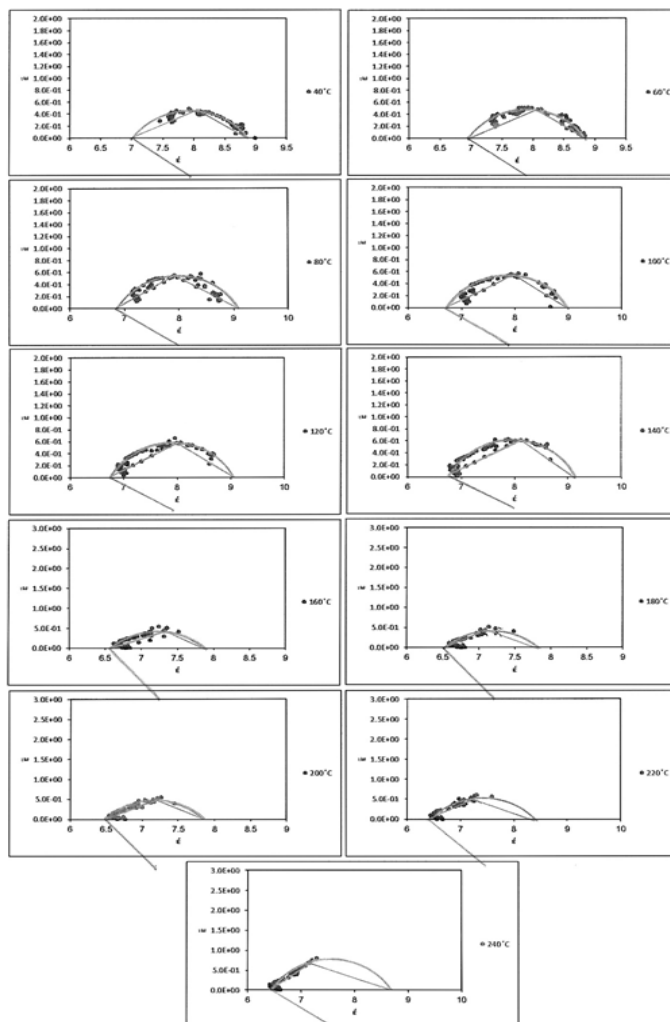


Figure 16: Cole-Cole diagrams for AD at different temperatures

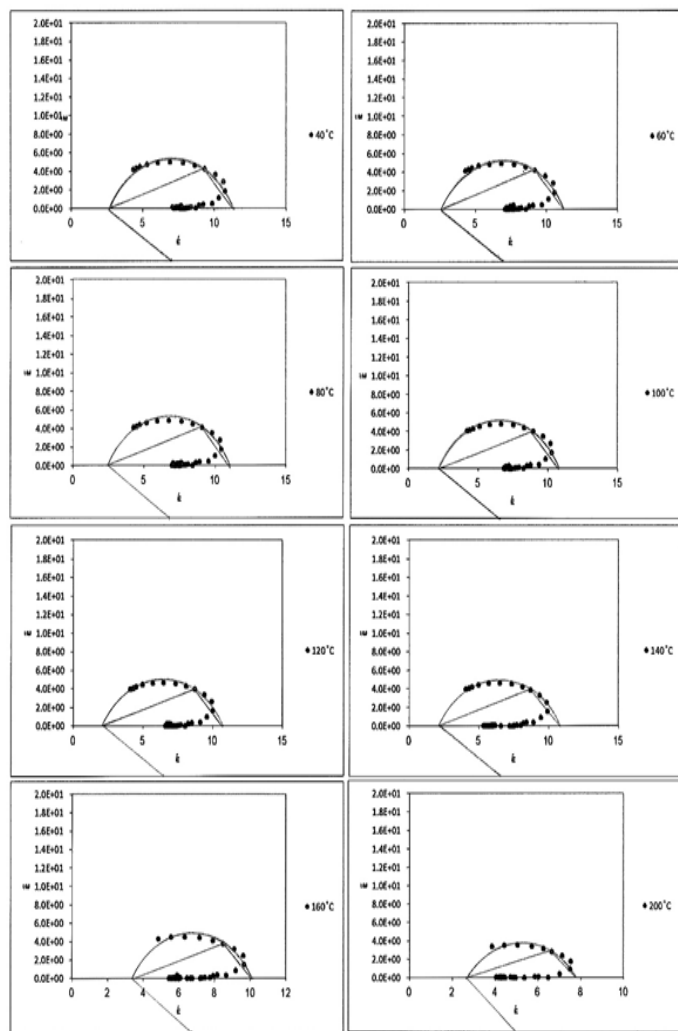
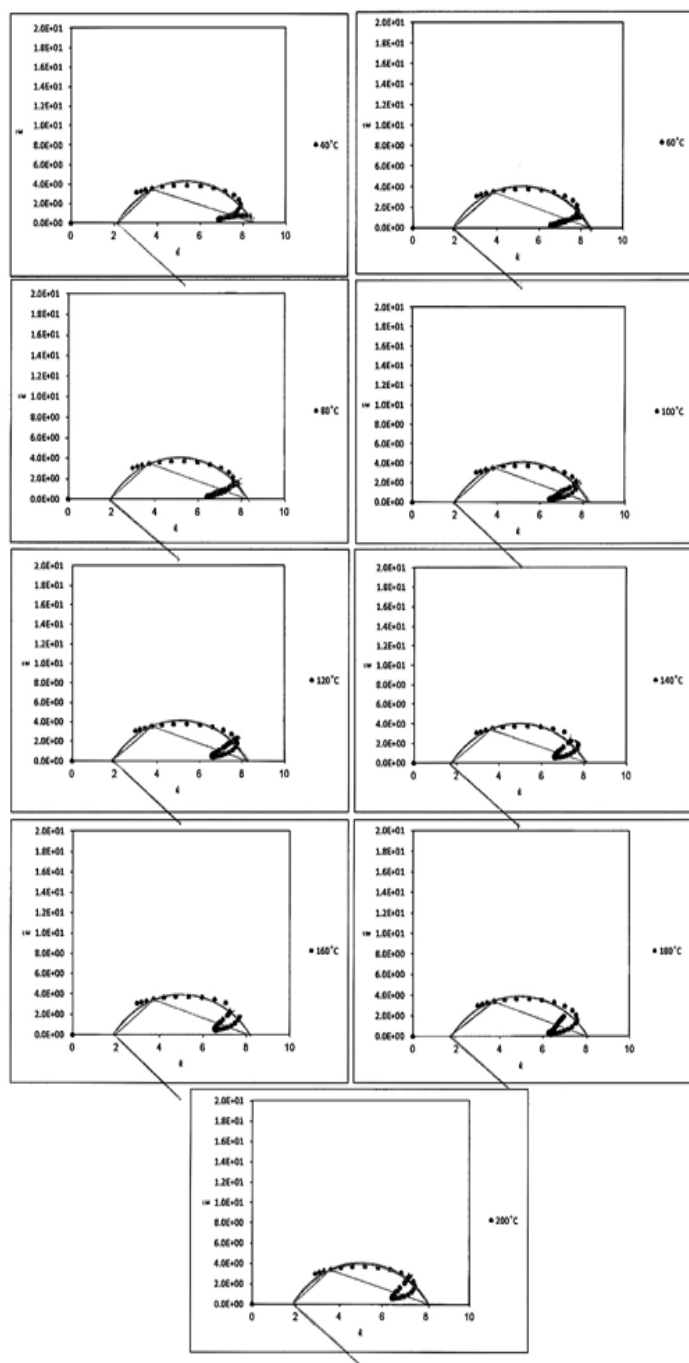


Figure 18: Cole-Cole diagrams for TBA at different temperatures

Figure 17: Cole-Cole diagrams for HEAD at different temperatures

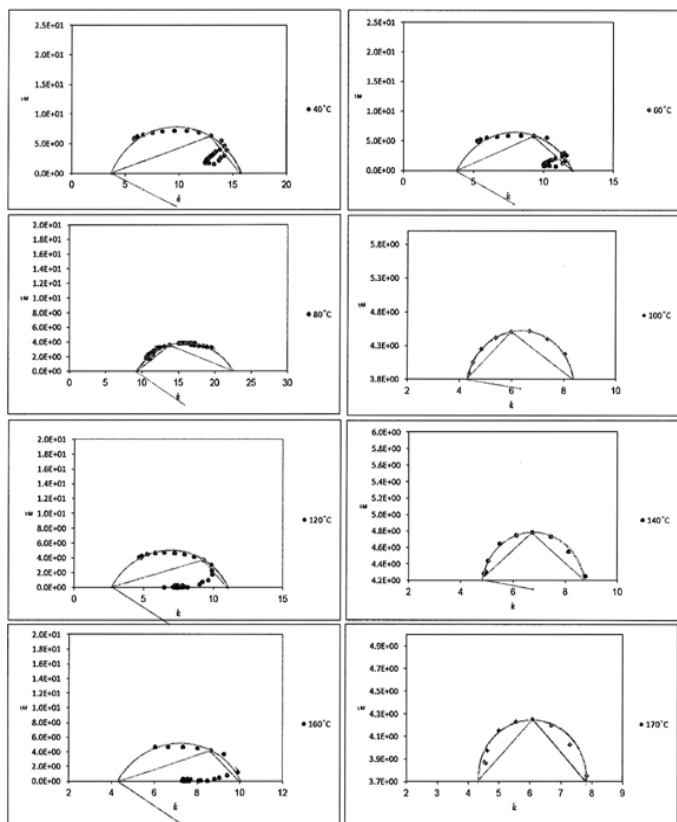


Figure 19: Cole-Cole diagrams for NBA at different temperatures

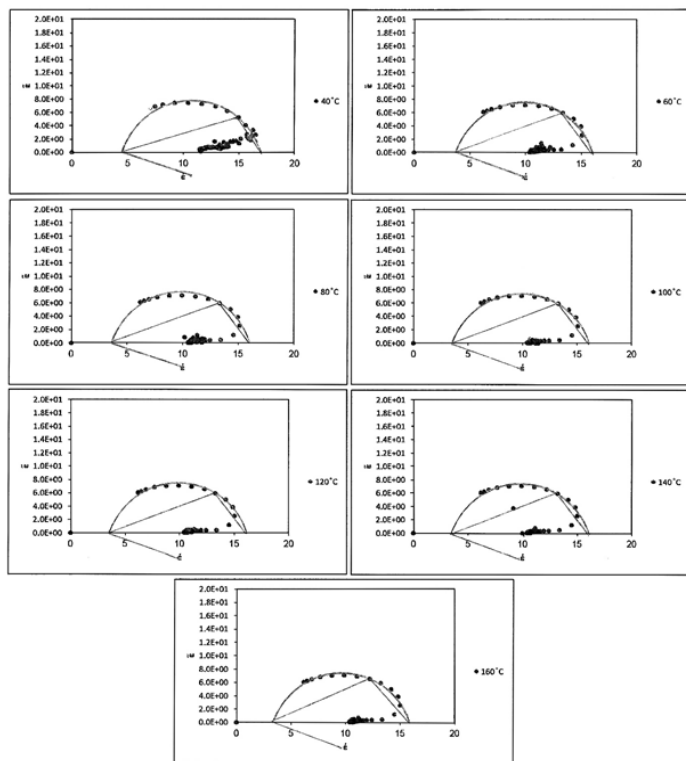


Figure 20: Cole-Cole diagrams for B at different temperatures

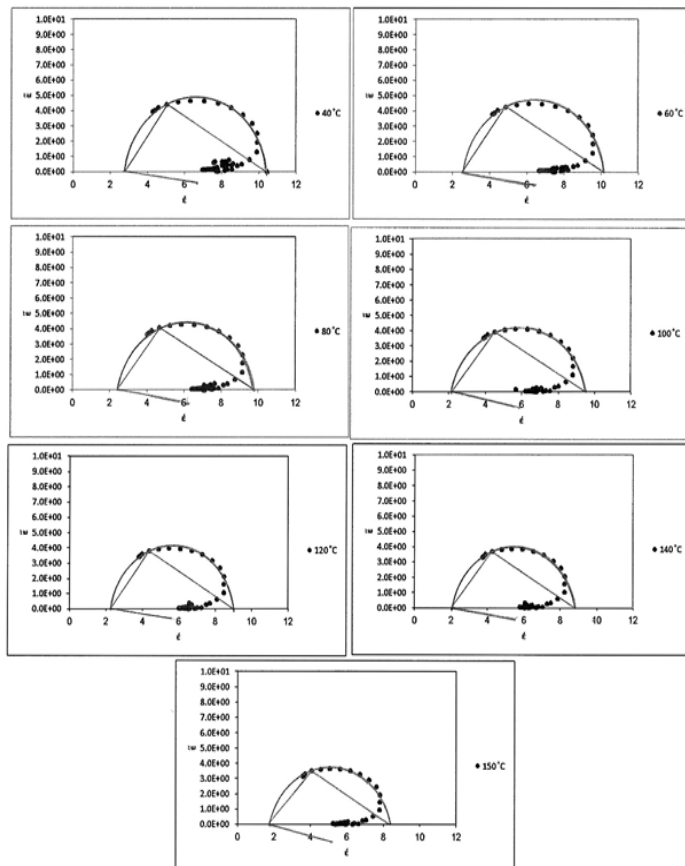


Figure 21: Cole-Cole diagrams for PB at different temperatures

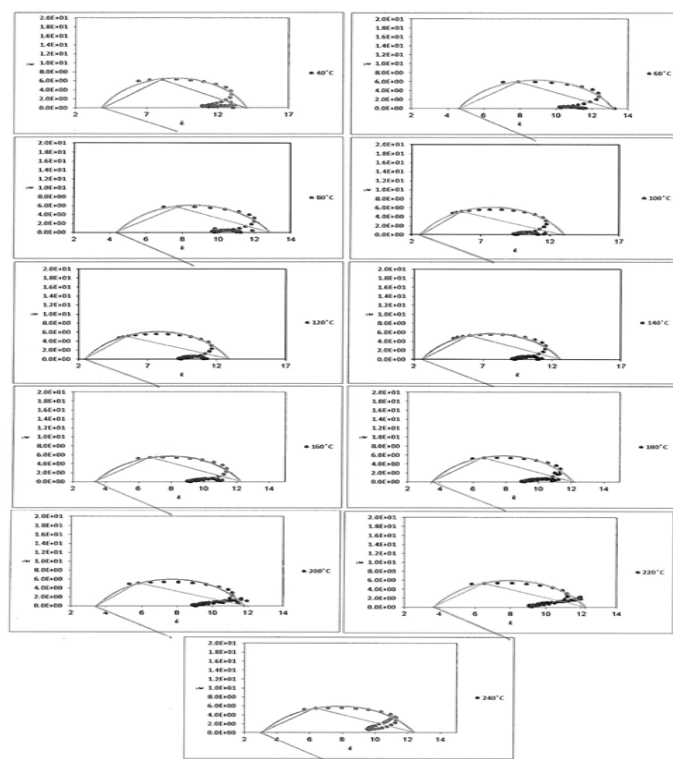


Figure 22: Cole-Cole diagrams for TU at different temperatures

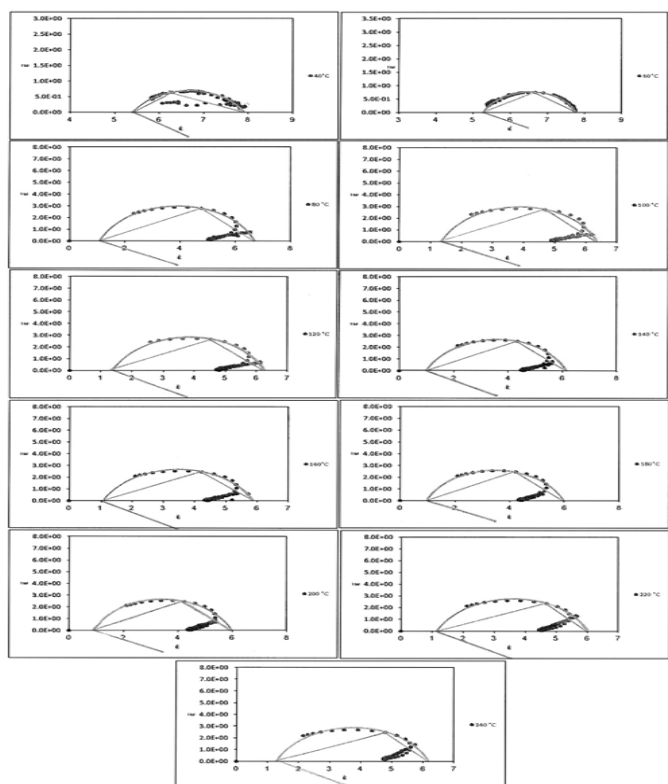


Figure 23: Cole-Cole diagrams for $\text{Hg}(\text{BA})_2$ at different temperatures

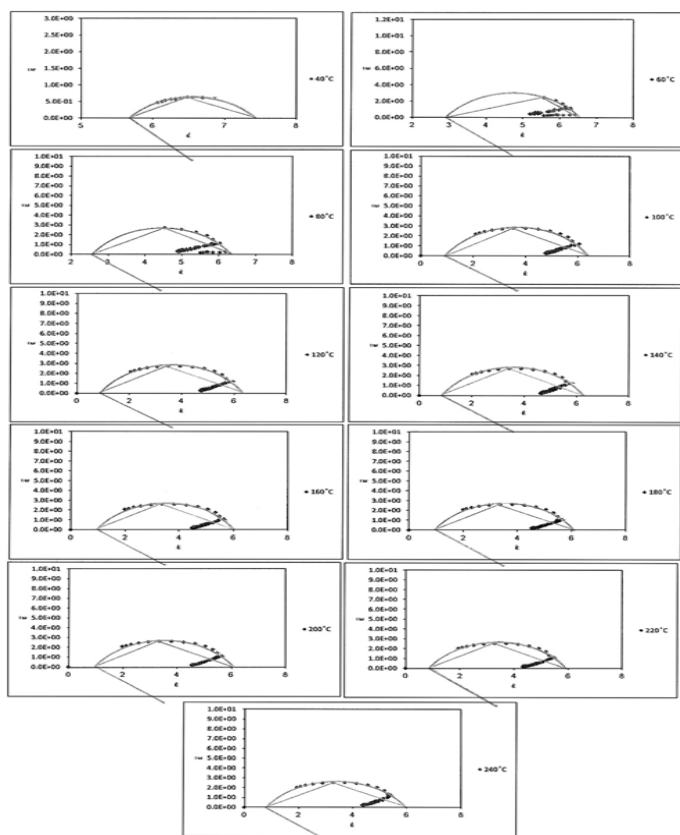


Figure 24: Cole-Cole diagrams for $\text{Cr}(\text{TU})(\text{OH})_2 \cdot \text{H}_2\text{O}$ at different temperatures

temperatures

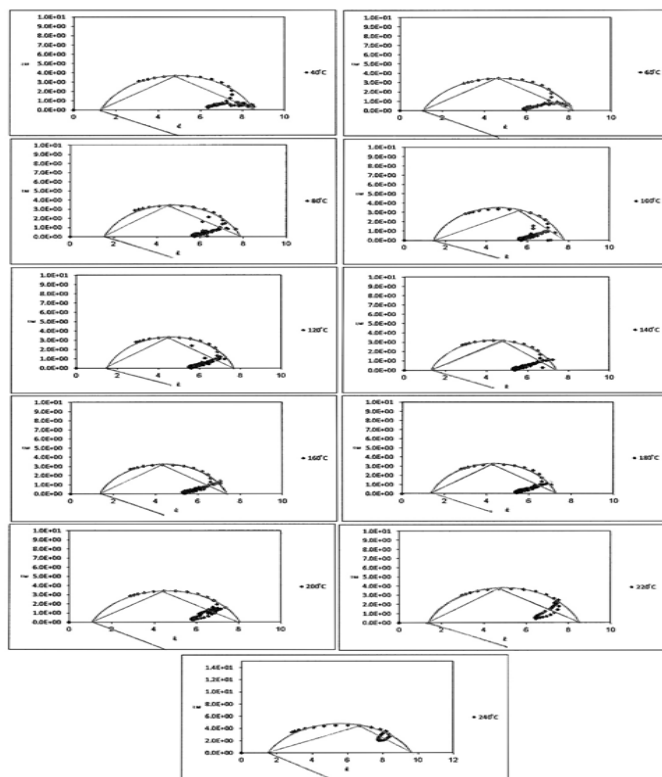


Figure 25: Cole-Cole diagrams for $\text{Mn}(\text{TU})_2 \cdot \text{H}_2\text{O}$ at different temperatures

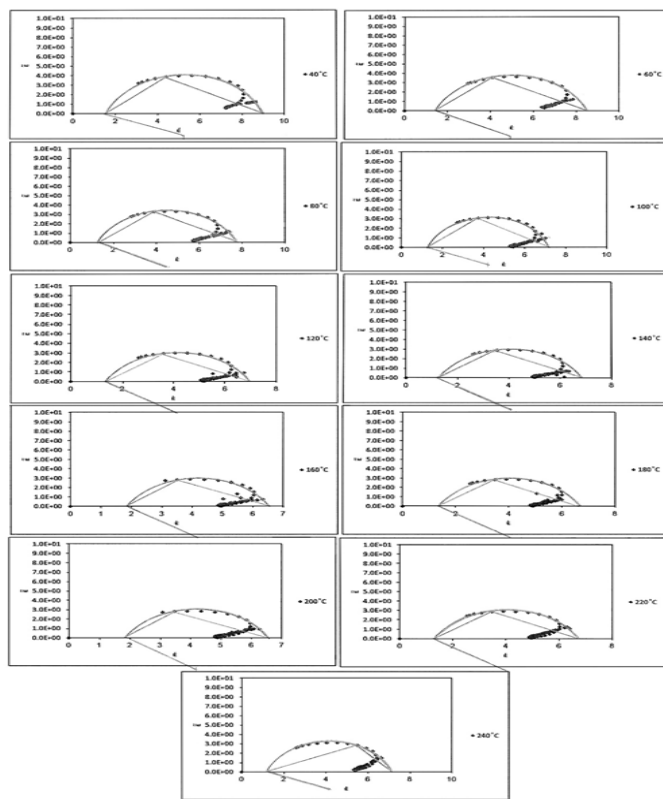


Figure 26: Cole-Cole diagrams for $\text{Co-Ni}(\text{TU})_3 \cdot 4\text{H}_2\text{O}$ at different temperatures

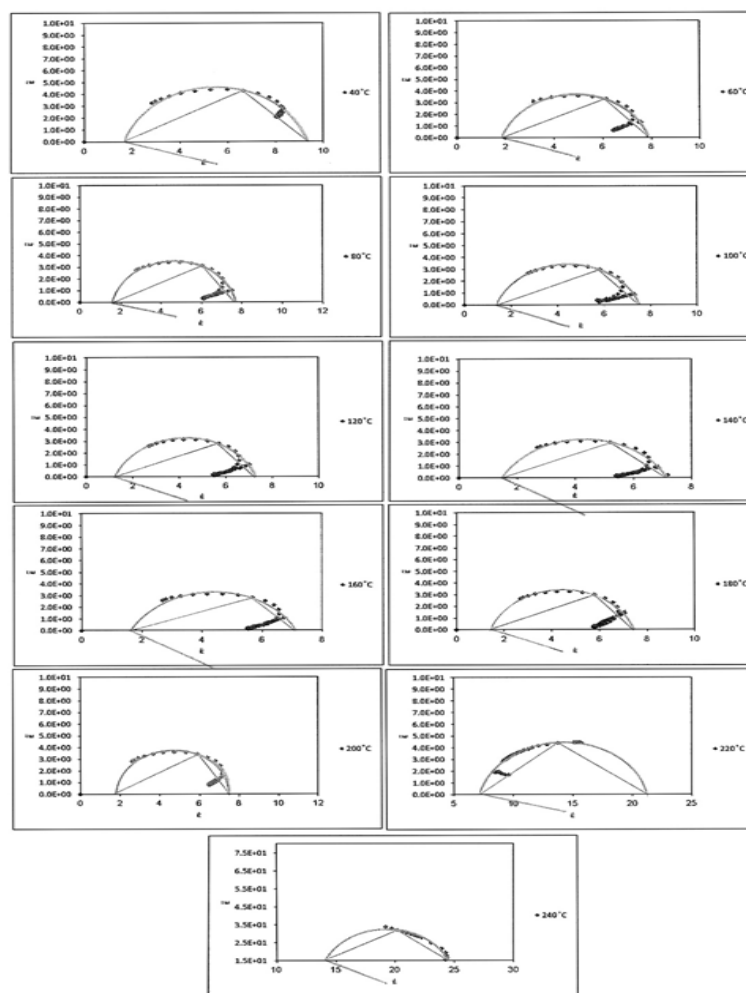


Figure 27: Cole-Cole diagrams for $\text{Hg(TU)}_2 \cdot 4\text{H}_2\text{O}$ at different temperatures

Table 3: The dielectric data obtained from the analysis of Cole-Cole diagrams for different compounds

| Compound | Temperature (K) | ω | ν | u | $\alpha \pi/2$ | α | $1 - \alpha$ | τ_0 | ϵ_s | ϵ_∞ | τ | $\ln \tau$ |
|----------|-----------------|----------|-------|------|----------------|----------|--------------------------|--------------------------|--------------|--------------------------|--------------------------|------------|
| AD | 313 | 345575.2 | 1.20 | 1.40 | 35 | 0.3889 | 0.6111 | 2.24858×10^{-6} | 8.85 | 7.00 | 2.09190×10^{-6} | -13.0774 |
| | 333 | 219911.5 | 1.20 | 1.50 | 35 | 0.3389 | 0.6111 | 3.15625×10^{-6} | 8.85 | 7.00 | 2.93633×10^{-6} | -12.7384 |
| | 353 | 113097.3 | 1.50 | 1.40 | 32.5 | 0.3611 | 0.6389 | 9.85023×10^{-6} | 9.09 | 6.82 | 9.03028×10^{-6} | -11.6149 |
| | 373 | 50265.5 | 1.30 | 1.50 | 31 | 0.3444 | 0.6556 | 1.59929×10^{-5} | 9.00 | 6.68 | 1.46187×10^{-5} | -11.1332 |
| | 393 | 31415.9 | 1.35 | 1.55 | 29 | 0.3222 | 0.6778 | 2.59614×10^{-5} | 9.05 | 6.73 | 2.37430×10^{-5} | -10.6482 |
| | 413 | 12566.4 | 1.35 | 1.65 | 28 | 0.3111 | 0.6889 | 5.94678×10^{-5} | 9.14 | 6.73 | 5.42410×10^{-5} | -9.82207 |
| | 433 | 25132.7 | 0.90 | 1.20 | 47.5 | 0.5278 | 0.4722 | 2.16363×10^{-5} | 7.93 | 6.57 | 2.03995×10^{-5} | -10.8000 |
| | 453 | 21991.1 | 1.10 | 0.90 | 47 | 0.5222 | 0.4778 | 6.92085×10^{-5} | 7.86 | 6.50 | 6.52168×10^{-5} | -9.63779 |
| | 473 | 18849.6 | 1.00 | 1.10 | 45 | 0.5000 | 0.5000 | 4.38443×10^{-5} | 7.86 | 6.50 | 4.13156×10^{-5} | -10.0943 |
| | 493 | 21991.1 | 1.40 | 0.90 | 42.5 | 0.4722 | 0.5278 | 1.05000×10^{-4} | 8.41 | 6.41 | 9.67067×10^{-5} | -9.24383 |
| 513 | 21991.1 | 1.80 | 0.95 | 32.5 | 0.3611 | 0.6389 | 1.24000×10^{-4} | 8.68 | 6.45 | 1.13000×10^{-4} | -9.08762 | |

Continued:

| | | | | | | | | | | | | |
|------|-----|------------|------|------|------|--------|--------|--------------------------|------|------|--------------------------|----------|
| HEAD | 313 | 27646015.4 | 2.20 | 0.90 | 37.5 | 0.4167 | 0.5833 | 1.67425×10^{-7} | 8.44 | 2.11 | 1.25568×10^{-7} | -15.8904 |
| | 333 | | 2.10 | 1.05 | 37.5 | 0.4167 | 0.5388 | 1.18691×10^{-7} | 8.44 | 2.00 | 8.85028×10^{-8} | -16.2402 |
| | 353 | | 2.10 | 1.00 | 35.5 | 0.3944 | 0.6056 | 1.23161×10^{-7} | 8.33 | 2.00 | 9.19641×10^{-8} | -16.2019 |
| | 373 | | 2.05 | 1.00 | 39.5 | 0.4389 | 0.5611 | 1.30007×10^{-7} | 8.33 | 2.00 | 9.70764×10^{-8} | -16.1478 |
| | 393 | | 2.10 | 1.00 | 39 | 0.4333 | 0.5667 | 1.33965×10^{-7} | 8.33 | 1.89 | 9.94414×10^{-8} | -16.1237 |
| | 413 | | 2.10 | 1.05 | 37.5 | 0.4167 | 0.5833 | 1.18691×10^{-7} | 8.11 | 1.78 | 8.78111×10^{-8} | -16.2481 |
| | 433 | | 2.10 | 1.00 | 40 | 0.4444 | 0.5556 | 1.37519×10^{-7} | 8.22 | 2.00 | 1.02832×10^{-7} | -16.0902 |
| | 453 | | 2.05 | 1.10 | 37.5 | 0.4167 | 0.5833 | 1.05158×10^{-7} | 8.11 | 1.78 | 7.77990×10^{-8} | -16.3691 |
| | 473 | | 2.10 | 1.00 | 37.5 | 0.4167 | 0.5833 | 1.29046×10^{-7} | 8.11 | 1.89 | 9.60549×10^{-8} | -16.1583 |

τ Ranges for AD and HEAD are (2.09190×10^{-6} - 1.13000×10^{-4} and 7.77990×10^{-8} - 1.25568×10^{-7}) respectively.

| Compound | Temperature (K) | ω | v | u | $\alpha \pi/2$ | α | $1 - \alpha$ | τ_0 | ϵ_s | ϵ_∞ | τ | $\ln \tau$ |
|----------|-----------------|------------|------|------|----------------|----------|--------------|--------------------------|--------------|-------------------|--------------------------|------------|
| TBA | 313 | 21362830.0 | 1.00 | 2.50 | 31 | 0.3444 | 0.6556 | 1.15695×10^{-8} | 11.39 | 2.78 | 8.65426×10^{-9} | -18.5652 |
| | 333 | | 1.00 | 2.45 | 31 | 0.3444 | 0.6556 | 1.19316×10^{-8} | 11.25 | 2.64 | 8.88770×10^{-9} | -18.5386 |
| | 353 | | 1.00 | 2.45 | 32 | 0.3556 | 0.6444 | 1.16537×10^{-8} | 11.11 | 2.36 | 8.59428×10^{-9} | -18.5722 |
| | 373 | | 1.00 | 2.45 | 30 | 0.3333 | 0.6667 | 1.22065×10^{-8} | 10.71 | 2.14 | 8.95069×10^{-9} | -18.5315 |
| | 393 | | 1.00 | 2.40 | 31 | 0.3444 | 0.6556 | 1.23128×10^{-8} | 10.71 | 2.14 | 9.02864×10^{-9} | -18.5229 |
| | 413 | | 1.00 | 2.40 | 31 | 0.3444 | 0.6556 | 1.23128×10^{-8} | 10.86 | 2.14 | 9.01732×10^{-9} | -18.5241 |
| | 433 | | 1.00 | 2.40 | 33 | 0.3667 | 0.6333 | 1.17492×10^{-8} | 10.11 | 3.44 | 9.16537×10^{-9} | -18.5078 |
| | 473 | | 0.80 | 2.20 | 38 | 0.4222 | 0.5778 | 8.12751×10^{-9} | 7.73 | 2.64 | 6.34360×10^{-9} | -18.8758 |
| NBA | 313 | 20106193.0 | 1.15 | 2.60 | 25 | 0.2778 | 0.7222 | 1.60744×10^{-8} | 15.74 | 3.70 | 1.19758×10^{-8} | -18.2404 |
| | 333 | 22619467.1 | 1.30 | 2.10 | 27.5 | 0.3056 | 0.6944 | 2.21616×10^{-8} | 12.14 | 3.82 | 1.70988×10^{-8} | -17.8843 |
| | 353 | 942477.8 | 1.70 | 1.00 | 32 | 0.3556 | 0.6444 | 2.41725×10^{-8} | 22.50 | 9.44 | 1.94956×10^{-6} | -13.1479 |
| | 373 | 25132741.2 | 1.90 | 1.55 | 8.5 | 0.0944 | 0.9056 | 4.98200×10^{-8} | 8.38 | 4.31 | 4.17545×10^{-8} | -16.9915 |
| | 393 | 20106193.0 | 0.90 | 2.35 | 30 | 0.3333 | 0.6667 | 1.17878×10^{-8} | 11.03 | 2.79 | 8.85241×10^{-9} | -18.5426 |
| | 413 | 25132741.2 | 1.70 | 1.65 | 9 | 0.1000 | 0.9000 | 4.11307×10^{-8} | 8.77 | 4.77 | 3.48774×10^{-8} | -17.1714 |
| | 433 | 21362830.0 | 1.00 | 2.40 | 31.5 | 0.3500 | 0.6500 | 1.21731×10^{-8} | 10.00 | 4.29 | 9.85615×10^{-9} | -18.4352 |
| | 443 | 25132741.2 | 1.95 | 1.95 | 0 | 0.0000 | 1.0000 | 3.97887×10^{-8} | 7.87 | 4.33 | 3.38230×10^{-8} | -17.2021 |
| B | 313 | 20106193.0 | 1.00 | 2.95 | 18 | 0.2000 | 0.8000 | 1.28645×10^{-8} | 17.04 | 4.44 | 9.69367×10^{-9} | -18.4518 |
| | 333 | | 1.20 | 2.75 | 20 | 0.2222 | 0.7778 | 1.61172×10^{-8} | 16.11 | 3.70 | 1.19787×10^{-8} | -18.2401 |
| | 353 | | 1.20 | 2.75 | 18.5 | 0.2056 | 0.7944 | 1.64818×10^{-8} | 16.11 | 3.52 | 1.21883×10^{-8} | -18.2228 |
| | 373 | 21362830.0 | 1.20 | 2.75 | 20 | 0.2222 | 0.7778 | 1.61172×10^{-8} | 16.11 | 3.52 | 1.19187×10^{-8} | -18.2452 |
| | 393 | | 1.20 | 2.75 | 20 | 0.2222 | 0.7778 | 1.61172×10^{-8} | 16.11 | 3.33 | 1.18553×10^{-8} | -18.2505 |
| | 413 | | 1.20 | 2.75 | 20 | 0.2222 | 0.7778 | 1.61172×10^{-8} | 16.11 | 3.33 | 1.18553×10^{-8} | -18.2505 |
| | 433 | 22619467.1 | 1.40 | 2.55 | 20 | 0.2222 | 0.7778 | 2.04504×10^{-8} | 15.93 | 3.33 | 1.50586×10^{-8} | -18.0113 |

τ Ranges for TBA, NBA and B are (6.34360×10^{-9} - 9.16537×10^{-9} , 8.85241×10^{-9} - 1.94956×10^{-6} and 9.69367×10^{-9} - 1.50586×10^{-8}) respectively.

| Compound | Temperature (K) | ω | v | u | $\alpha \pi/2$ | α | $1 - \alpha$ | τ_0 | ϵ_s | ϵ_∞ | τ | $\ln \tau$ |
|----------|-----------------|------------|------|------|----------------|----------|--------------|--------------------------|--------------|-------------------|--------------------------|------------|
| PB | 313 | 27646015.4 | 2.60 | 1.60 | 8 | 0.0889 | 0.9111 | 6.16300×10^{-8} | 10.35 | 2.71 | 4.64656×10^{-8} | -16.8846 |
| | 333 | | 2.60 | 1.60 | 8 | 0.0889 | 0.9111 | 6.16300×10^{-8} | 10.12 | 2.47 | 4.61007×10^{-8} | -16.8924 |
| | 353 | | 2.50 | 1.50 | 10 | 0.1111 | 0.8889 | 6.42610×10^{-8} | 9.76 | 2.35 | 4.79982×10^{-8} | -16.8521 |
| | 373 | | 2.40 | 1.50 | 10 | 0.1111 | 0.8889 | 6.13765×10^{-8} | 9.53 | 2.12 | 4.54689×10^{-8} | -16.9062 |

Continued:

| | | | | | | | | | | | | |
|----|-----|------------|------|------|------|--------|--------|--------------------------|-------|------|--------------------------|----------|
| | 393 | | 2.20 | 1.40 | 8.5 | 0.0944 | 0.9056 | 5.95847×10^{-8} | 9.06 | 2.24 | 4.46337×10^{-8} | -16.9248 |
| | 413 | | 2.20 | 1.40 | 8 | 0.0889 | 0.9111 | 5.94036×10^{-8} | 8.82 | 2.00 | 4.40925×10^{-8} | -16.937 |
| | 423 | | 2.10 | 1.40 | 13.5 | 0.1500 | 0.8500 | 5.82819×10^{-8} | 8.35 | 1.76 | 4.29495×10^{-8} | -16.9632 |
| TU | 313 | 25132741.2 | 1.85 | 1.40 | 25 | 0.2778 | 0.7222 | 5.85274×10^{-8} | 14.14 | 3.96 | 4.44819×10^{-8} | -16.9282 |
| | 333 | 25132741.2 | 2.00 | 1.40 | 32 | 0.3556 | 0.6444 | 6.92031×10^{-8} | 13.29 | 4.57 | 5.40676×10^{-8} | -16.733 |
| | 353 | 25132741.2 | 1.95 | 1.40 | 32.5 | 0.3611 | 0.6389 | 6.68352×10^{-8} | 12.86 | 4.43 | 5.22312×10^{-8} | -16.7676 |
| | 373 | 28902652.4 | 2.10 | 1.05 | 30 | 0.3333 | 0.6667 | 9.78605×10^{-8} | 12.93 | 2.56 | 7.16988×10^{-8} | -16.4508 |
| | 393 | 28902652.4 | 2.10 | 1.05 | 29 | 0.3222 | 0.6778 | 9.62066×10^{-8} | 12.93 | 2.37 | 7.00158×10^{-8} | -16.4745 |
| | 413 | 27646015.4 | 1.90 | 1.15 | 30 | 0.3333 | 0.6667 | 7.68159×10^{-8} | 12.56 | 2.56 | 5.64295×10^{-8} | -16.6903 |
| | 433 | 26389378.3 | 1.90 | 1.25 | 33 | 0.3667 | 0.6333 | 7.33994×10^{-8} | 12.31 | 3.38 | 5.56507×10^{-8} | -16.7042 |
| | 453 | 26389378.3 | 1.90 | 1.25 | 30 | 0.3333 | 0.6667 | 7.10127×10^{-8} | 12.31 | 3.54 | 5.41489×10^{-8} | -16.7315 |
| | 473 | 27646015.4 | 2.20 | 1.05 | 31 | 0.3444 | 0.6556 | 1.11785×10^{-7} | 11.86 | 3.43 | 8.52999×10^{-8} | -16.2771 |
| | 493 | 26389378.3 | 2.10 | 1.20 | 32.5 | 0.3611 | 0.6389 | 9.09868×10^{-8} | 12.29 | 3.57 | 6.94678×10^{-8} | -16.4824 |
| | 513 | 26389378.3 | 2.00 | 1.30 | 32.5 | 0.3611 | 0.6389 | 7.43707×10^{-8} | 12.31 | 3.08 | 5.57831×10^{-8} | -16.7018 |

τ Ranges for PB and TU are (4.29495×10^{-8} - 4.79982×10^{-8} and 4.44819×10^{-8} - 8.52999×10^{-8}) respectively.

| Compound | Temperature (K) | ω | ν | u | $\alpha \pi/2$ | α | $1 - \alpha$ | τ_0 | ϵ_s | ϵ_∞ | τ | $\ln \tau$ |
|---|-----------------|------------|-------|------|----------------|----------|--------------------------|--------------------------|--------------|--------------------------|--------------------------|------------|
| Hg(BA) ₂ | 313 | 942477.8 | 1.60 | 1.00 | 32.5 | 0.3611 | 0.6389 | 2.21422×10^{-6} | 7.89 | 5.42 | 1.98316×10^{-6} | -13.1308 |
| | 333 | 125663.7 | 1.05 | 1.30 | 26 | 0.2889 | 0.7111 | 5.89325×10^{-6} | 7.75 | 5.25 | 5.25957×10^{-6} | -12.1555 |
| | 353 | 22619467.1 | 1.50 | 2.30 | 24 | 0.2667 | 0.7333 | 2.46818×10^{-8} | 6.66 | 1.08 | 1.77887×10^{-8} | -17.8447 |
| | 373 | | 1.50 | 2.35 | 24 | 0.2667 | 0.7333 | 2.39685×10^{-8} | 6.38 | 1.38 | 1.77071×10^{-8} | -17.8493 |
| | 393 | | 1.50 | 2.30 | 27 | 0.3000 | 0.7000 | 2.40062×10^{-8} | 6.31 | 1.38 | 1.77542×10^{-8} | -17.8466 |
| | 413 | | 1.40 | 2.10 | 27 | 0.3000 | 0.7000 | 2.47719×10^{-8} | 6.17 | 0.96 | 1.77993×10^{-8} | -17.8441 |
| | 433 | | 1.40 | 2.25 | 28 | 0.3111 | 0.6889 | 2.22027×10^{-8} | 5.92 | 1.00 | 1.60520×10^{-8} | -17.9474 |
| | 453 | | 1.35 | 2.05 | 23 | 0.2556 | 0.7444 | 2.52243×10^{-8} | 6.00 | 0.96 | 1.81615×10^{-8} | -17.824 |
| | 473 | | 1.30 | 2.05 | 24 | 0.2667 | 0.7333 | 2.37561×10^{-8} | 6.00 | 0.87 | 1.69856×10^{-8} | -17.8909 |
| | 493 | 21362830.0 | 1.20 | 2.45 | 27.5 | 0.3056 | 0.6944 | 1.6748×10^{-8} | 6.00 | 1.15 | 1.22353×10^{-8} | -18.2189 |
| | 513 | 21362830.0 | 1.25 | 2.40 | 27.5 | 0.3056 | 0.6944 | 1.82973×10^{-8} | 6.15 | 1.31 | 1.34974×10^{-8} | -18.1208 |
| Cr(TU)(OH) ₂ .H ₂ O | 313 | 25132741.2 | 1.50 | 1.30 | 43.5 | 0.4833 | 0.5167 | 5.24864×10^{-8} | 7.43 | 5.66 | 4.83185×10^{-8} | -16.8455 |
| | 333 | 20106193.0 | 0.95 | 2.10 | 37 | 0.4111 | 0.5889 | 1.29324×10^{-8} | 6.53 | 2.93 | 1.05558×10^{-8} | -18.3666 |
| | 353 | 22619467.1 | 1.55 | 1.70 | 35 | 0.3889 | 0.6111 | 3.80077×10^{-8} | 6.33 | 2.53 | 3.04021×10^{-8} | -17.3088 |
| | 373 | 25132741.2 | 1.75 | 1.60 | 32.5 | 0.3611 | 0.6389 | 4.578×10^{-8} | 6.36 | 0.91 | 3.27034×10^{-8} | -17.2358 |
| | 393 | 25132741.2 | 1.75 | 1.60 | 33 | 0.3667 | 0.6333 | 4.58363×10^{-8} | 6.36 | 0.91 | 3.27437×10^{-8} | -17.2346 |
| | 413 | 25132741.2 | 1.75 | 1.60 | 35 | 0.3889 | 0.6111 | 4.60728×10^{-8} | 6.27 | 0.82 | 3.27237×10^{-8} | -17.2352 |
| | 433 | 25132741.2 | 1.70 | 1.50 | 35 | 0.3889 | 0.6111 | 4.88325×10^{-8} | 6.00 | 1.00 | 3.52679×10^{-8} | -17.1603 |
| | 453 | 25132741.2 | 1.70 | 1.50 | 35 | 0.3889 | 0.6111 | 4.88325×10^{-8} | 6.09 | 0.91 | 3.49873×10^{-8} | -17.1683 |
| | 473 | 25132741.2 | 1.70 | 1.50 | 35 | 0.3889 | 0.6111 | 4.88325×10^{-8} | 6.09 | 1.00 | 3.52278×10^{-8} | -17.1614 |
| | 493 | 25132741.2 | 1.70 | 1.50 | 36 | 0.4000 | 0.6000 | 4.90181×10^{-8} | 6.00 | 0.91 | 3.51569×10^{-8} | -17.1634 |
| 513 | 25132741.2 | 1.70 | 1.50 | 36 | 0.4000 | 0.6000 | 4.90181×10^{-8} | 6.00 | 0.82 | 3.49118×10^{-8} | -17.1704 | |

τ Ranges for Hg(BA)₂ and Cr-(TU)(OH)₂.H₂O are (1.22353×10^{-8} - 5.25957×10^{-6} and 1.05558×10^{-8} - 4.83185×10^{-8}) respectively.

Continued:

| Compound | Temperature (K) | ω | v | u | $\alpha \pi/2$ | α | 1 - α | τ_0 | ϵ_s | ϵ_∞ | τ | ln τ |
|---|-----------------|------------|------|------|----------------|----------|--------------|--------------------------|--------------|-------------------|--------------------------|-----------|
| Mn (TU) ₂ .H ₂ O | 313 | 25132741.2 | 1.90 | 1.85 | 25 | 0.2778 | 0.7222 | 4.12854×10 ⁻⁸ | 8.56 | 1.33 | 2.96618×10 ⁻⁸ | -17.3334 |
| | 333 | 25132741.2 | 1.90 | 1.85 | 26 | 0.2889 | 0.7111 | 4.13092×10 ⁻⁸ | 8.22 | 1.11 | 2.93989×10 ⁻⁸ | -17.3423 |
| | 353 | 25132741.2 | 1.75 | 1.65 | 23 | 0.2556 | 0.7444 | 4.30612×10 ⁻⁸ | 7.89 | 1.56 | 3.15455×10 ⁻⁸ | -17.2718 |
| | 373 | 22619467.1 | 1.30 | 2.00 | 20 | 0.2222 | 0.7778 | 2.54084×10 ⁻⁸ | 7.88 | 1.41 | 1.84544×10 ⁻⁸ | -17.808 |
| | 393 | 25132741.2 | 1.65 | 1.60 | 20 | 0.2222 | 0.7778 | 4.13945×10 ⁻⁸ | 7.76 | 1.53 | 3.03168×10 ⁻⁸ | -17.3116 |
| | 413 | 23876104.2 | 1.40 | 1.70 | 22.5 | 0.2500 | 0.7500 | 3.23302×10 ⁻⁸ | 7.41 | 1.41 | 2.36041×10 ⁻⁸ | -17.5618 |
| | 433 | 25132741.2 | 1.60 | 1.55 | 25 | 0.2778 | 0.7222 | 4.15769×10 ⁻⁸ | 7.44 | 1.44 | 3.04003×10 ⁻⁸ | -17.3088 |
| | 453 | 25132741.2 | 1.60 | 1.55 | 24 | 0.2667 | 0.7333 | 4.15492×10 ⁻⁸ | 7.33 | 1.44 | 3.04203×10 ⁻⁸ | -17.3082 |
| | 473 | 25132741.2 | 1.85 | 1.75 | 28 | 0.3111 | 0.6889 | 4.31313×10 ⁻⁸ | 8.11 | 1.11 | 3.07220×10 ⁻⁸ | -17.2983 |
| | 493 | 25132741.2 | 2.00 | 1.80 | 28 | 0.3111 | 0.6889 | 4.63642×10 ⁻⁸ | 8.56 | 1.33 | 3.33107×10 ⁻⁸ | -17.2174 |
| | 513 | 21362830.0 | 1.35 | 2.10 | 30 | 0.3333 | 0.6667 | 2.41275×10 ⁻⁸ | 9.73 | 1.47 | 1.73001×10 ⁻⁸ | -17.8726 |
| Co-Ni (TU) ₃ .4H ₂ O | 313 | 26389378.3 | 2.30 | 1.70 | 20 | 0.2222 | 0.7778 | 5.58931×10 ⁻⁸ | 9.00 | 1.56 | 4.04914×10 ⁻⁸ | -17.0222 |
| | 333 | | 2.20 | 1.55 | 25 | 0.2778 | 0.7222 | 6.15401×10 ⁻⁸ | 8.56 | 1.44 | 4.44776×10 ⁻⁸ | -16.9283 |
| | 353 | | 2.00 | 1.45 | 25 | 0.2778 | 0.7222 | 5.91492×10 ⁻⁸ | 7.89 | 1.33 | 4.27564×10 ⁻⁸ | -16.9677 |
| | 373 | | 1.70 | 1.40 | 20 | 0.2222 | 0.7778 | 4.86389×10 ⁻⁸ | 7.29 | 1.29 | 3.52949×10 ⁻⁸ | -17.1595 |
| | 393 | | 2.00 | 1.45 | 30.5 | 0.3389 | 0.6611 | 6.16346×10 ⁻⁸ | 6.91 | 1.36 | 4.51333×10 ⁻⁸ | -16.9136 |
| | 413 | | 1.95 | 1.50 | 30 | 0.3333 | 0.6667 | 5.61676×10 ⁻⁸ | 6.91 | 1.18 | 4.06423×10 ⁻⁸ | -17.0185 |
| | 433 | | 2.10 | 1.30 | 31 | 0.3444 | 0.6556 | 7.87553×10 ⁻⁸ | 6.54 | 1.85 | 5.99295×10 ⁻⁸ | -16.6301 |
| | 453 | | 1.95 | 1.40 | 30 | 0.3333 | 0.6667 | 6.22918×10 ⁻⁸ | 6.73 | 1.36 | 4.57238×10 ⁻⁸ | -16.9006 |
| | 473 | | 2.15 | 1.25 | 31 | 0.3444 | 0.6556 | 8.66666×10 ⁻⁸ | 6.62 | 1.85 | 6.58509×10 ⁻⁸ | -16.5359 |
| | 493 | | 2.00 | 1.45 | 31 | 0.3444 | 0.6556 | 6.18892×10 ⁻⁸ | 6.73 | 1.27 | 4.51524×10 ⁻⁸ | -16.9132 |
| | 513 | 21362830.0 | 1.10 | 2.00 | 20 | 0.2222 | 0.7778 | 2.17031×10 ⁻⁸ | 7.22 | 1.22 | 1.56912×10 ⁻⁸ | -17.9702 |
| τ Ranges for Mn(TU) ₂ .H ₂ O and Co-Ni(TU) ₃ .4H ₂ O are (1.73001×10 ⁻⁸ - 3.33107×10 ⁻⁸ and 1.56912×10 ⁻⁸ - 6.58509×10 ⁻⁸) respectively. | | | | | | | | | | | | |
| Compound | Temperature (K) | ω | v | u | $\alpha \pi/2$ | α | 1 - α | τ_0 | ϵ_s | ϵ_∞ | τ | ln τ |
| Hg (TU) ₂ .4H ₂ O | 313 | 21362830.0 | 1.70 | 2.50 | 16 | 0.1778 | 0.8222 | 2.92844×10 ⁻⁸ | 9.33 | 1.67 | 2.12701×10 ⁻⁸ | -17.666 |
| | 333 | | 1.20 | 2.10 | 17 | 0.1889 | 0.8111 | 2.34804×10 ⁻⁸ | 7.89 | 1.89 | 1.75285×10 ⁻⁸ | -17.8594 |
| | 353 | | 1.05 | 1.90 | 15 | 0.1667 | 0.8333 | 2.29755×10 ⁻⁸ | 7.73 | 1.60 | 1.69022×10 ⁻⁸ | -17.8958 |
| | 373 | | 1.10 | 2.10 | 20 | 0.2222 | 0.7778 | 2.03835×10 ⁻⁸ | 7.53 | 1.41 | 1.48613×10 ⁻⁸ | -18.0245 |
| | 393 | | 1.10 | 2.10 | 22.5 | 0.2500 | 0.7500 | 1.97654×10 ⁻⁸ | 7.29 | 1.18 | 1.42434×10 ⁻⁸ | -18.067 |
| | 413 | | 1.30 | 2.20 | 30 | 0.3333 | 0.6667 | 2.12629×10 ⁻⁸ | 7.18 | 1.45 | 1.56066×10 ⁻⁸ | -17.9756 |
| | 433 | | 1.10 | 2.40 | 30 | 0.3333 | 0.6667 | 1.45249×10 ⁻⁸ | 7.18 | 1.64 | 1.07892×10 ⁻⁸ | -18.3447 |
| | 453 | | 1.10 | 2.10 | 21 | 0.2333 | 0.7667 | 2.01394×10 ⁻⁸ | 7.44 | 1.44 | 1.47256×10 ⁻⁸ | -18.0337 |
| | 473 | | 1.10 | 1.80 | 0 | 0.0000 | 1.0000 | 2.86063×10 ⁻⁸ | 7.47 | 1.73 | 2.12792×10 ⁻⁸ | -17.6655 |
| | 493 | 942477.8 | 2.10 | 1.90 | 14 | 0.1556 | 0.8444 | 1.19454×10 ⁻⁶ | 21.14 | 7.05 | 9.29151×10 ⁻⁷ | -13.889 |
| | 513 | 4398.2 | 1.20 | 1.50 | 25 | 0.2778 | 0.7222 | 1.67000×10 ⁻⁴ | 24.55 | 14.09 | 1.43000×10 ⁻⁴ | -8.8511 |
| τ Ranges for Hg(TU) ₂ .4H ₂ O is (1.07892×10 ⁻⁸ - 1.43000×10 ⁻⁴) . | | | | | | | | | | | | |

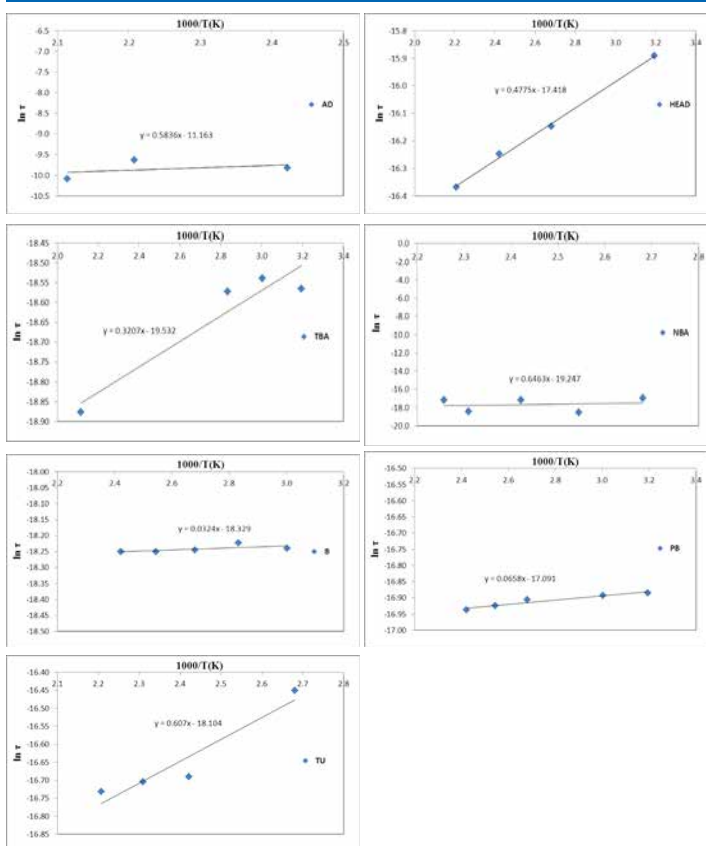


Figure 28: $\ln \tau$ -1000/T relationship for ligands

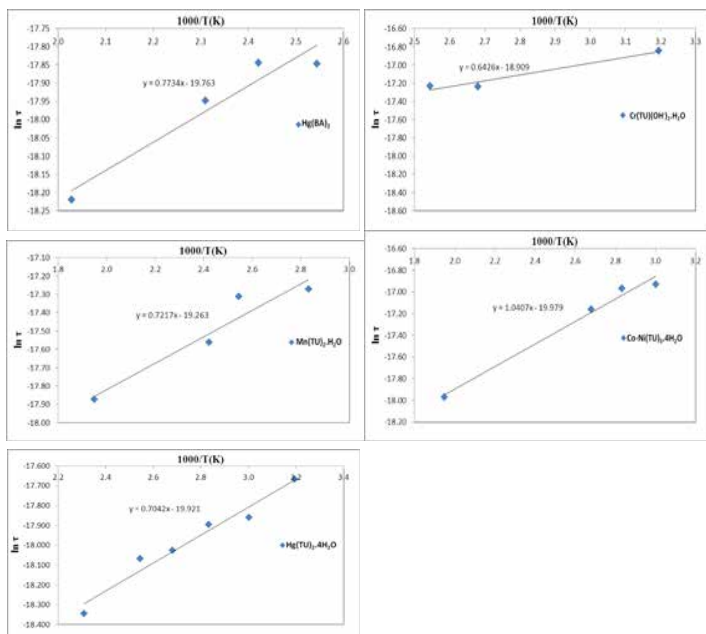


Figure 29: $\ln \tau$ -1000/T relationship for complexes

Table 4: The activation energies E_0 (kJ mol⁻¹) for the relaxation processes of compounds

| Compound | E_0 (kJ mol ⁻¹) |
|---|-------------------------------|
| AD | 4.85 |
| HEAD | 3.97 |
| TBA | 2.66 |
| NBA | 5.37 |
| B | 0.27 |
| PB | 0.54 |
| TU | 5.05 |
| Hg(BA) ₂ | 6.43 |
| Cr(TU)(OH) ₂ .H ₂ O | 5.34 |
| Mn(TU) ₂ .H ₂ O | 5.99 |
| Co-Ni(TU) ₃ .4H ₂ O | 8.65 |
| Hg(TU) ₂ .4H ₂ O | 5.85 |

Electrical Conductivity Measurements

The alternating current conductivity (σ) is calculated according to the following equation [10]:

$$\sigma \text{ (}\Omega^{-1} \text{ cm}^{-1}\text{)} = \omega \times C_p \text{ (pF)} \times \tan \delta \times \frac{d}{A} \text{ (cm}^{-1}\text{)} \times 10^{-12}$$

The frequency dependence of a. c. conductivity for ligands and complexes at different temperatures is illustrated in Figures (30, 31). The behavior shows that the a. c. conductivity gradually increases with increasing the frequency. At lower frequencies the grain boundaries are more effective than grains in electrical conduction hence the hopping of ions are bound at lower frequencies. As the frequency of the applied field increases the conductive grains become more active and promote the conduction mechanism [25].

From the practical standpoint, materials may be classified according to their conductivities into three categories [14]:

Conductivity range

- i. Conductors 10^6 - $10^8 \Omega^{-1} \text{ m}^{-1}$
- ii. Semiconductors 10^5 - $10^7 \Omega^{-1} \text{ m}^{-1}$
- iii. Insulators 10^{-8} - $10^{-20} \Omega^{-1} \text{ m}^{-1}$

However, the conductivity of the conductors decreases with increasing temperature whilst that of semiconductors and insulators increases with increasing temperature [14].

In the present ligands and complexes, the conductivities have a magnitude close to that of semiconductors, where the electrons in

the orbitals are not of sufficient mobility to be promoted [26-33]. The study of the conduction mechanism of organic materials leads to an increasing use of these materials in commercial devices such as solar energy panels, scintillation counter and also in some technological applications such as photocopy process [34].

The investigation of electron transport in disorder systems has been gradually developed.

The investigation of gap states is of particular interest, because of their effect on the electrical properties of semiconductor materials [35, 36]. Several concepts proposed by many workers start from the premise that the contribution of carriers hopping between localized states to electrical conductivity is expected in amorphous semiconductors [37-39]. The hopping conduction can be easily distinguished from that of the band conduction by measuring the frequency dependence of conductivity, which as expected, is due to conduction in localized states [39-42].

Theories proposed for a.c. conduction in amorphous semiconductors have mostly assumed that carrier motion occurs through quantum mechanical tunneling (QMT) between localized states near the Fermi-level [43, 44].

The classification of organic compounds on the basis of semiconducting properties was originally proposed by Garrett [45]. This classification consisted of polymers, charge transfer (CT) complexes and molecular crystals. Another mode of classification was given to four groups [46]: (i) molecular crystals bonded by relatively weak Van der Waals forces, (ii) complexes which also exhibit, in addition to the Van der Waals interaction, a varying degree of covalent and coordinate bonding, (iii) polymers which are really macromolecules held together by ionic and covalent bonding, and (iv) free radicals or their salts.

Eley proposed a theory of charge carrier formation and migration in organic semiconductor based on simplified assumption that the electron should tunnel from the first excited molecular orbital through a conductivity of levels [47-49]. Hansel model for electrical conduction mechanism of organic solids is based on [50]:

1. The conductivity depends on the mobility of π -electrons.
2. In the molecule, the π -electrons are localized in the molecule framework and their delocalization requires activation energy.
3. The delocalized π -electrons migrate to the neighbouring molecule by tunnel effect. As the temperature increases, the bonds are exhausted resulting in an increase of the conductivity.

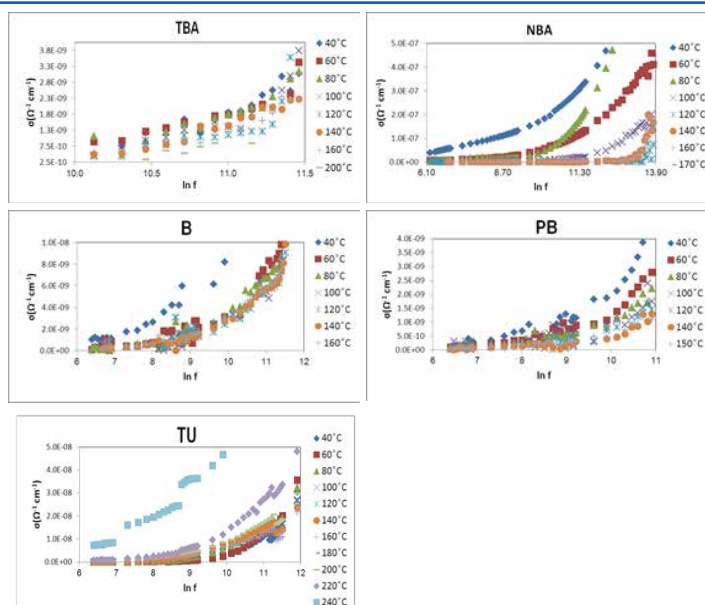
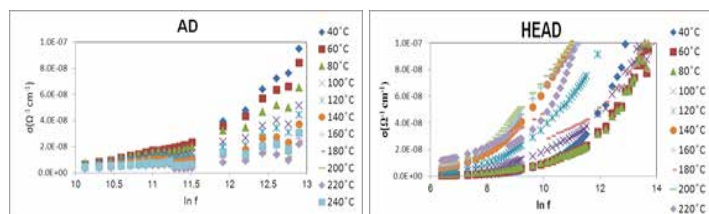


Figure 30: A.C. conductivity σ - $\ln f$ relationship for ligands at different temperatures

Figure 31: A.C. conductivity σ - $\ln f$ relationship for complexes at different temperatures \blacktriangle 40°C, \blacksquare 60°C, \blacktriangle 80°C, \times 100°C, \times 120°C, \blacktriangle 140°C, \blacktriangle 160°C, \blacktriangle 180°C, \blacktriangle 200°C, \blacktriangle 220°C and \blacktriangle 240°C

The electrical conductivity of substances at a given frequency varies exponentially with the absolute temperature according to the Arrhenius relation [51]:

$$\sigma = \sigma_0 e^{-\Delta E/kT}$$

where σ is the electrical conductivity at an absolute temperature T , σ_0 is the pre-exponential factor, ΔE is the activation energy.

Therefore, the temperature dependence of the electrical conductivity is characterized by the two constants: the activation energy (ΔE) and the pre-exponential factor (σ_0).

The variations of $\ln \sigma$ as a function of reciprocal absolute temperature for ligands and complexes at different frequencies are illustrated in Figures (32, 33). The activation energy data and $\ln \sigma_0$ values for ligands and complexes are given in Table (5).

A discontinuity in the conductivity curve at a transition temperature can be ascribed to a molecular rearrangement or different crystallographic or phase transitions [52, 53]. The magnitude of the conductivities along with the values of the energy gaps indicated slight semiconducting properties. The most realistic description of the complex involves an interaction of the metal orbitals with the ligands to give new molecular orbitals (MO), which are delocalized over the whole molecular complex. In view of the high degree of covalency in the M-O and M-N bonds, it is no longer permissible to distinguish the central metal from the ligands. The complexes must be regarded as individual entities.

The experimental results of a.c. conductivity σ , have been analyzed in terms of various theoretical models. Application of correlated barrier-hopping (CBH) model reveals that electronic conduction takes place by bipolaron or mixed polaron hopping process [54].

The relationship between molecular structure and electrical properties was deduced [55, 56]. On the basis of electronic transition within molecules, two pathways for the conduction of electricity may be expected [57]. The first conducting process occurring in the lower temperature region is attributed to $n \rightarrow \pi^*$ transitions which require less energy to be performed. In the upper temperature region, conduction could be attributed to $\pi \rightarrow \pi^*$ transitions which need more energy to participate in electronic conduction. The observed increment of conduction in the upper temperature region may be attributed to interactions between $n \rightarrow \pi^*$ and $\pi \rightarrow \pi^*$ transitions.

The lower temperature range is the region of extrinsic semiconductor where the conduction is due to the excitation of carriers from donor localized level to the conduction band. In the upper temperature range, the intrinsic region is reached where carriers are thermally activated from the valence band to the conduction band [58]. This behavior can be explained as follows: the upper temperature range may be attributed to the interaction between the electrons of d-orbitals and the p-orbitals of the ligand [59]. This interaction will lead to small delocalization of the p-electronic charge on the ligand which tends to increase the activation energy. The presence of d-electrons in a narrow energy band leads to magnetic ordering and degeneracy of d-bands with respect to the orbital quantum number, which is only partially lifted in a crystal field [60, 61].

In all ligands and complexes, during thermal agitation, an additional increase in electrical conductivity occurs, which probably indicating a discontinuity of the chemical bonds existing in the

structure. This is a useful criterion for ascertaining the nature of the metal-ligand bonding [62].

It is found that the activation energy decreased with increasing the atomic number of the metal in the $Mn(TU)_2 \cdot H_2O$ and $Hg(TU)_2 \cdot 4H_2O$ complexes, which indicates that the presence of holes in the system has little effect on the mobility of charges [63, 64].

For the complexes, the metal ion forms a bridge with the ligands, thus facilitating the transfer of current carriers with some degree of delocalization in the excited state during measurements. Meanwhile, this leads to an increase of the electrical conductivity with a decrease in energy of activation [65].

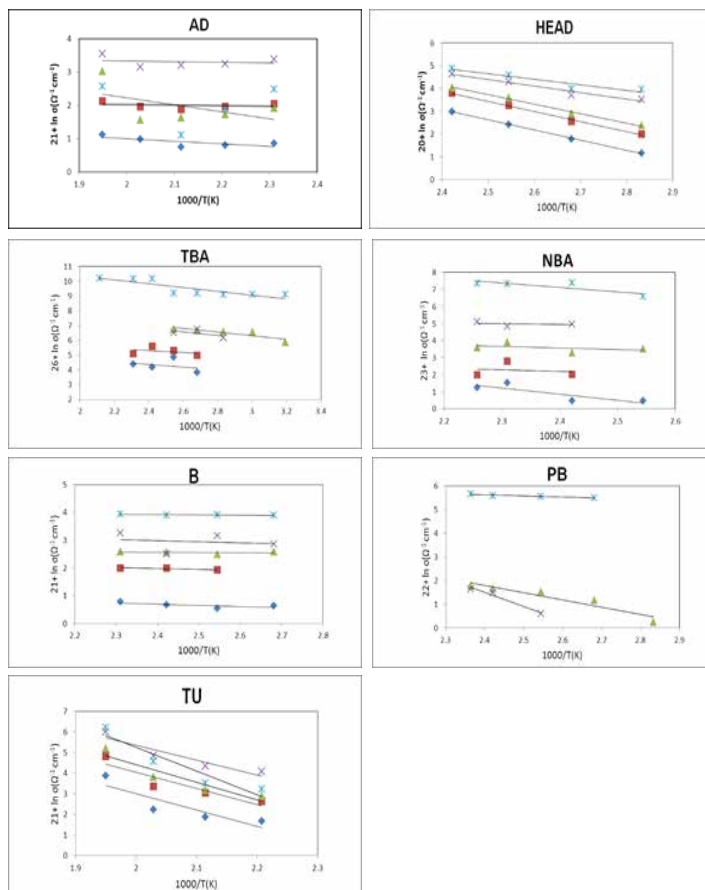
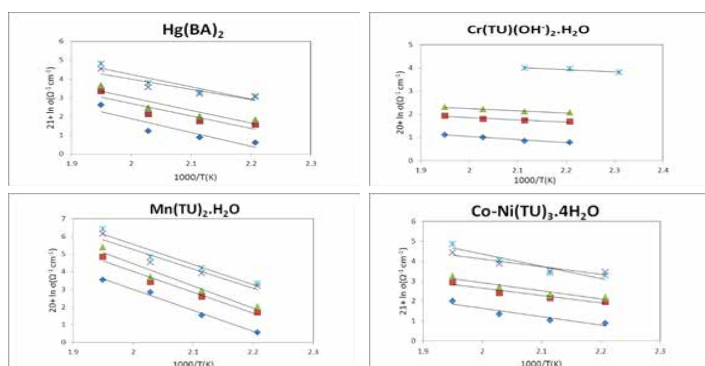


Figure 32: $\ln \sigma - 1000/T$ relationship for ligands at different frequencies \bullet 10 kHz, \blacksquare 50 kHz, \blacktriangle 100 kHz, \blacklozenge 500 kHz and \times 1000 kHz



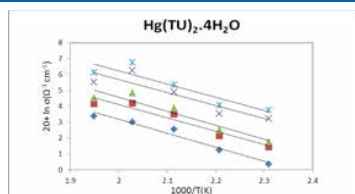


Figure 33: $\ln \sigma_0 - 1000/T$ relationship for complexes at different frequencies \bullet 10 kHz, \blacksquare 50 kHz, \blacktriangle 100 kHz, \blacklozenge 500 kHz and \times 1000 kHz

Table 5: The activation energy data ΔE (kJ mol⁻¹) and $\ln \sigma_0$ values for compounds at different frequencies

| Compound | Frequency(kHz) | $\ln \sigma_0$ | ΔE (kJ mol ⁻¹) |
|----------|----------------|----------------|------------------------------------|
| AD | 10 | -18.50 | 6.24 |
| | 50 | -18.66 | 1.33 |
| | 100 | -14.57 | 17.43 |
| | 500 | -17.27 | 1.67 |
| | 1000 | -18.67 | 1.20 |
| HEAD | 10 | -6.23 | 37.09 |
| | 50 | -5.51 | 36.78 |
| | 100 | -5.87 | 34.61 |
| | 500 | -8.46 | 23.79 |
| | 1000 | -9.28 | 20.22 |
| TBA | 10 | -19.53 | 7.23 |
| | 50 | -19.19 | 5.22 |
| | 100 | -15.95 | 10.36 |
| | 500 | -16.32 | 9.89 |
| | 1000 | -13.09 | 10.63 |
| NBA | 10 | -13.55 | 29.70 |
| | 50 | -18.43 | 8.23 |
| | 100 | -17.29 | 7.45 |
| | 500 | -16.93 | 3.92 |
| | 1000 | -9.69 | 21.43 |
| B | 10 | -19.22 | 3.76 |
| | 50 | -18.31 | 2.49 |
| | 100 | -18.28 | 0.56 |
| | 500 | -17.12 | 3.14 |
| | 1000 | -16.90 | 0.62 |
| PB | 100 | -12.90 | 25.36 |
| | 500 | -6.10 | 49.88 |
| | 1000 | -15.17 | 4.16 |
| TU | 10 | -2.18 | 65.78 |
| | 50 | -1.23 | 65.38 |
| | 100 | 0.55 | 71.27 |
| | 500 | -1.21 | 60.04 |
| | 1000 | 7.25 | 95.70 |

Continued:

| Compound | Frequency(kHz) | ln σ_0 | ΔE (kJ mol ⁻¹) |
|---|----------------|---------------|------------------------------------|
| Hg(BA) ₂ | 10 | -4.47 | 60.91 |
| | 50 | -5.13 | 54.84 |
| | 100 | -4.44 | 56.39 |
| | 500 | -6.06 | 45.55 |
| | 1000 | -3.71 | 54.32 |
| Cr(TU)(OH) ₂ .H ₂ O | 10 | -16.33 | 10.97 |
| | 50 | -16.21 | 8.02 |
| | 100 | -15.84 | 7.96 |
| | 1000 | -15.78 | 8.18 |
| Mn(TU) ₂ .H ₂ O | 10 | 6.88 | 99.23 |
| | 50 | 7.70 | 98.40 |
| | 100 | 9.66 | 104.81 |
| | 500 | 7.26 | 91.40 |
| | 1000 | 8.36 | 94.82 |
| Co-Ni(TU) ₃ .4H ₂ O | 10 | -11.01 | 34.78 |
| | 50 | -10.96 | 30.76 |
| | 100 | -10.02 | 33.58 |
| | 500 | -9.23 | 31.86 |
| | 1000 | -4.39 | 50.94 |
| Hg(TU) ₂ .4H ₂ O | 10 | 0.76 | 73.11 |
| | 50 | 0.87 | 69.70 |
| | 100 | 2.20 | 73.30 |
| | 500 | 2.03 | 67.99 |
| | 1000 | 2.84 | 69.11 |

Molecular Modeling

The molecular modeling calculations are widely increasing nowadays for the expectation of the mechanism of the reactions and the identification of the products [66].

This saves time and money. The multidentate ligands including nitrogen, sulphur and oxygen atoms are versatile and useful for assembly new molecules, because they can coordinate many transition metal ions. Thus, the syntheses and structures of new complexes are significant for understanding the biological phenomena and exploiting artificial models [67].

Also, a theoretical support for the experimental findings regarding the donor atoms could be obtained on comparing the molecular models of the complexes with that of the free ligands.

For example the molecular modeling calculations of the compounds BA and Hg(BA)₂, Figures (34, 35) (a(ChemOffice modeling), b(HyperChem modeling)) are given concerning the bond lengths, bond angles, dihedral angles and HyperChem data. These calculations are based on using molecular orbital package (MOPAC) for minimizing energies where the Austin Model 1(AM1) method is used, also Parameterized Model 3(PM3) is applied for HyperChem.

Quantum chemical parameters such as the highest occupied molecular orbital energy (E_{HOMO}) and the lowest unoccupied molecular orbital energy (E_{LUMO}) were given using HyperChem modeling, where energy gap (ΔE) and parameters which give information about the reactive chemical behavior of compounds such as electronegativity (χ), chemical potential (μ), global hardness (η), softness (σ) and electrophilicity index (ω) were calculated, Table (6).

$$\Delta E = E_{\text{LUMO}} - E_{\text{HOMO}}$$

The concepts of these parameters are related to each other, the energies of the (HOMO) and (LUMO) orbitals of the molecule are related to ionization potential (I) and the electron affinity (A), respectively, and their relations with χ and μ are given by the following equations [68-72]:

$$I = -E_{\text{HOMO}} \quad \mu = -\chi$$

$$A = -E_{\text{LUMO}} \quad \mu = \frac{-(I+A)}{2} = \frac{E_{\text{HOMO}} + E_{\text{LUMO}}}{2}$$

Large χ values characterize acids and small χ values are found for bases.

The qualitative definition of hardness is related to the polarizability, because a decrease of the energy gap usually leads to an easier polarization of the molecule [68].

$$\eta = \frac{I-A}{2} = \frac{E_{\text{LUMO}} - E_{\text{HOMO}}}{2}$$

The inverse of the hardness is equal to softness, (σ) as follows:

$$\sigma = \frac{1}{\eta}$$

The energy difference between the HOMO and LUMO (HOMO-LUMO gap) can be used to predict the strength and stability of transition metal complexes.

Hard molecules have a large HOMO-LUMO gap while, soft molecules have a small HOMO-LUMO gap.

Soft molecules have small excitation energies to the excited states, therefore they will be more polarizable and more reactive than the hard molecules.

Hard molecules resist changes in their electron number and distribution.

The electrophilicity index (ω) in terms of chemical potential (μ) and hardness (η) is given from the equation [73-75]:

$$\omega = \frac{\mu^2}{2\eta}$$

BA, TBA and B have a largest values of χ , Table (6).

HOMO-LUMO gap is decreased and softness increased upon complexation with BA ligand, which give stabilization for complex formation.

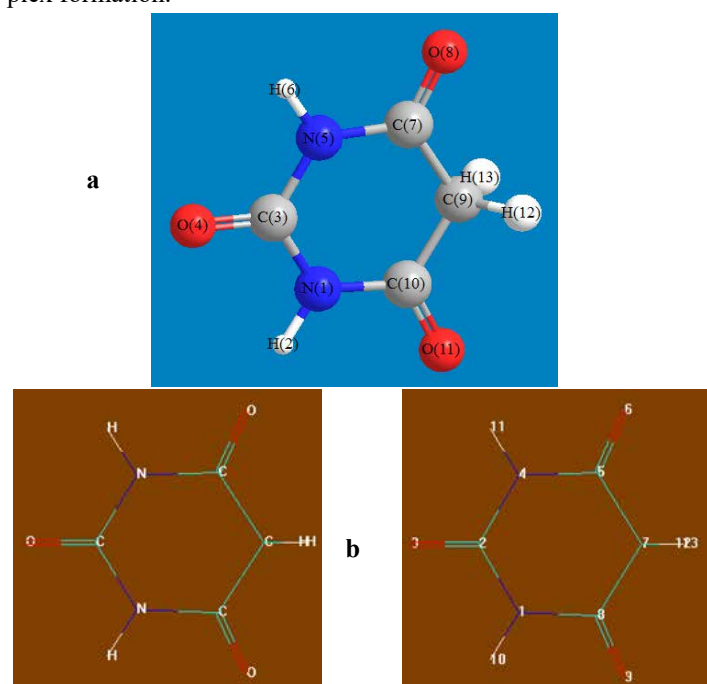


Figure 34: The molecular modeling of Barbituric acid (BA), a)

ChemOffice, b) HyperChem

HyperChem Calculations

Total energy: -40174.049 (kcal/mol).

Binding energy: -1420.823 (kcal/mol).

Isolated atomic energy: -38753.226 (kcal/mol).

Electronic energy: -165585.243 (kcal/mol).

Core-core interaction: 125411.193 (kcal/mol).

Heat of formation: -124.178(kcal/mol).

Dipole moment: 0.810 Debye.

HOMO: -10.828eV; **LUMO:** -0.421eV.

Net charges of atoms: (1(-0.024), 2 (0.230), 3(-0.361), 4(-0.024), 5(0.251), 6(-0.334), 7(-0.145), 8(0.251), 9(-0.334),10(0.127),11(0.127),12 (0.117) and 13(0.118)).

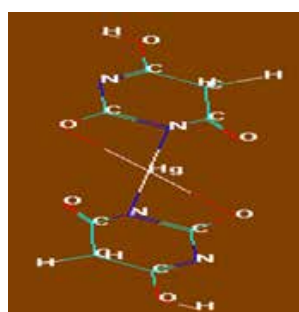
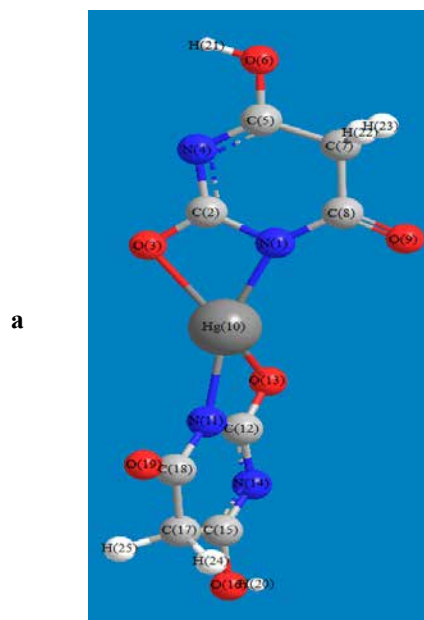


Figure 35: The molecular modeling of Hg(BA)₂, a) ChemOffice, b) HyperChem

HyperChem Calculations

Total energy: -80283.147 (kcal/mol).

Binding energy: -2713.185 (kcal/mol).

Isolated atomic energy: -77569.963 (kcal/mol).

Electronic energy: -447712.500 (kcal/mol).

Core-core interaction: 367429.353 (kcal/mol).

Heat of formation: -209.409 (kcal/mol).

Dipole moment: 3.087 Debye.

HOMO: -10.030eV; **LUMO:** -0.652eV.

Net charges of atoms: (1(-0.317), 2(0.328), 3(-0.343), 4(-0.251), 5(0.168), 6(-0.229), 7(-0.097), 8(0.283), 9(-0.369), 10(0.745), 11(-0.317), 12(0.327), 13(-0.343), 14(-0.251), 15(0.168), 16(-0.229), 17(-0.097), 18(0.283), 19(-0.369), 20(0.237), 21(0.237), 22(0.111), 23(0.109), 24(0.111) and 25(0.109)).

Table 6: Quantum chemical parameters (eV) of compounds calculated by PM3 method

| Compound | E_{HOMO} | E_{LUMO} | $\Delta E = (E_{\text{L}} - E_{\text{H}})$ | χ | μ | η | σ | ω |
|--|-------------------|-------------------|--|--------|---------|--------|----------|----------|
| AD | -8.557 | -0.234 | 8.323 | 4.3955 | -4.3955 | 4.1615 | 0.2403 | 2.3213 |
| HEAD | -8.778 | -0.411 | 8.367 | 4.5945 | -4.5945 | 4.1835 | 0.2390 | 2.5229 |
| BA | -10.828 | -0.421 | 10.407 | 5.6245 | -5.6245 | 5.2035 | 0.1922 | 3.0398 |
| Hg(BA) ₂ | -10.030 | -0.652 | 9.378 | 5.3410 | -5.3410 | 4.6890 | 0.2133 | 3.0418 |
| TBA | -9.529 | -1.750 | 7.779 | 5.6395 | -5.6395 | 3.8895 | 0.2571 | 4.0884 |
| B | -10.761 | -0.328 | 10.433 | 5.5445 | -5.5445 | 5.2165 | 0.1917 | 2.9466 |
| PB | -8.388 | -1.077 | 7.311 | 4.7325 | -4.7325 | 3.6555 | 0.2736 | 3.0634 |
| TU | -9.278 | -1.343 | 7.935 | 5.3105 | -5.3105 | 3.9675 | 0.2520 | 3.5541 |
| Hg(TU) ₂ .4H ₂ O | -9.251 | -1.265 | 7.986 | 5.2580 | -5.2580 | 3.9930 | 0.2504 | 3.4619 |

References

- GE Pike (1972) ac Conductivity of Scandium Oxide and a New Hopping Model for Conductivity. Phys Rev, B6, 1572, Philos B Mag 1972: 6.
- SR Elliott (1977) A theory of a.c. conduction in chalcogenide glasses. Philos Mag 36: 1291-1304.
- SS Kim and WJ Kim (2005) Electrical properties of sol-gel derived pyrochlore-type bismuth magnesium niobate Bi₂(Mg_{1/3}Nb_{2/3})₂O₇ thin films. J Crystal Growth 281: 432-439.
- PS Anantha and K Hariharan (2005) ac Conductivity analysis and dielectric relaxation behaviour of NaNO₃-Al₂O₃ composites. J Materials Science and Engineering B 121: 12-19.
- HM Zaki (2005) AC conductivity and frequency dependence of the dielectric properties for copper doped magnetite. J Physica B: Condensed Matter 363: 232-244.
- M Okutan, E Basaran, HI Bakan and F Yakuphanoglu (2005) AC conductivity and dielectric properties of Co-doped TiO₂. J Physica B: Condensed Matter 364: 300-305.
- AA Hendi (2011) AC Conductivity and Dielectric Measurements of Bulk Tertracyanoquinodimethane. Aust J Basic& Appl Sci 5: 380-386.
- W Brütting (2004) Physics of Organic Semiconductors. Phys Stat Solidi A 201: 1035.
- A Vogel (2004) Textbook of Quantitative Chemical Analysis. 4th Indian Reprint.
- AK Jonscher (1983) Dielectric Relaxation in Solids. Chelsea Dielectric, London.
- JS Blakemore (1995) Solid State Physics. 2nd Ed, Cambridge Univ Press.
- HM Rosenberg (1997) The Solid State. 3rd Ed, Oxford Univ Press.
- H Fröhlich (1949) Theory of Dielectrics. Oxford Univ Press, London.
- AA Zaky and R Hawley (1970) Dielectric Solids. Routledge and Kegan Paul Ltd, London, UK.
- A Vasudevan, S Carin, MR Melloch, ES Harmon (1998) Permittivity of GaAs epilayers containing arsenic precipitates. Appl Phys Lett 73: 671.
- HM Lin, YF Chen, JL Shen and WC Chou (2001) Dielectric studies of Cd_{1-x-y}Zn_xMn_yTe crystals. J Appl Phys 89: 4476-4479.
- B Tareev (1979) Physics of Dielectric Materials. Mir Publishers, Moscow.
- S Kurien, J Mathew, S Sebastian, SNPotty and KC George (2006) Dielectric behavior and ac electrical conductivity of nanocrystalline nickel aluminate. Mater Chem Phys 98: 470-476.
- JM Thomas (1977) Prospects in solid state chemistry. Chemistry in Britain 13: 175-182.
- MM Ahmad, K Yamada and T Okuda (2002) Frequency dependent conductivity and dielectric studies on RbSn₂F₅. Solid State Communications 123: 185-189.
- VV Daniel (1967) Dielectric Relaxation. Academic Press, London and New York.
- KS Cole and RH Cole (1941) Dispersion and Absorption in Dielectrics I. Alternating Current Characteristics. J Chem Phys 9: 341.
- MS Masoud, AE Ali, RH Mohamed and M Abd El-Zaher Mostafa (2005) Dielectric relaxation Spectroscopy of heteronuclear cobalt(II) copper(II) complex of 1-phenyl-3-methyl-5-pyrazolone. Spectrochim Acta 62: 1114-1119.
- E Şentürk (2004) Dielectric characteristics of Ce³⁺ doped Sr_{0.61}Ba_{0.39}Nb₂O₆ with Cole-Cole plots technique. Cryst Res Technol 39: 157-160.
- K Verma, A Kumar and D Varshney (2012) Dielectric relaxation behavior of A_xCo_{1-x}Fe₂O₄ (A = Zn, Mg) mixed ferrites. J Alloys Compd 526: 91-97.
- MS Masoud, ME Kassem, Y Abd El-Aziz and S Massoud (1987) Electrical conductivity of some azo complexes containing sulphur. Xth Conference on Solid State Science and Applications 1987: 46.
- TM Salem, MM Osman, MS Masoud, MF El-Shazly, MM

- Abou-Sekkina (1979) Electrical conductivity mechanisms in inorganic solids. *Al Physica* 2: 43.
28. MS Masoud, BS Farag, YA Sawan, TM Salem and MM El-Esawy (1983) Electrical conductivity of 2,4-dinitrosoresorcinol and its complexes. *J Non-Crystalline Solids* 55: 209-213.
 29. A El-Dessouky, A El-Sonbati and M Kassem (1986) Metal chelates of heterocyclic nitrogen-containing ketones: XVII. effect of temperature and gamma irradiation on the electrical conductivity of 2-quinaldyl phenyl ketone and its metal complexes. *Thermochim Acta* 103: 213.
 30. MS Masoud, ME Kassem, S Hedewy and AR Youssef (1987) Conducting properties of 3-amino-4-(substituted phenylazo)-5-(1H)-pyrazolone ligands and their complexes. 1st Regional Symposium of Materials Science (In the Arab States), Alex.
 31. MS Masoud, EM Soliman and M El-Shabasy (1988) Effect of temperature on the electrical conductivity of some 4-(substituted)-3-hydroxy-2-quinoline ligands and their complexes. *Thermochim Acta* 125: 9-16.
 32. MS Masoud, A El-Khatib, M Kassem and AR Youssef (1988) Effect of Fast Neutron Irradiation on the Electrical conductivity of Some Azo Pyrazolones at Different Temperatures. *J Mater Sci Lett* 7: 1291-1294.
 33. MS Masoud, GB Mohamed, ME Kassem, A El-Dessouky, AM Hindawy, et al. (1990) Temperature-electrical conductivity relations for 5-nitro- and 6-nitrobenzimidazole and their transition metal complexes. *Thermochim Acta* 159: 215-223.
 34. AT Vartanyan (1947) *Acta Phys Chem. USSR* 22: 201.
 35. W Beyer, H Mell, J Stuke (1971) Conductivity and Thermoelectric Power of Trigonal Se_xTe_{1-x} Single Crystals. *J Phys Status Sol* 45: 153-162.
 36. AI Gubanov (1965) Quantum electron theory of amorphous conductors. consultants Bureau.
 37. MH Cohen, H Fritzsche and SR Ovshinsky (1969) Simple Band Model for Amorphous Semiconducting Alloys. *Phys Rev Lett* 22: 1065.
 38. EA Davis and NF Mott (1970) Conduction in non-crystalline systems V. Conductivity, optical absorption and photoconductivity in amorphous semiconductors. *Phil Mag* 22: 903-922.
 39. M Pollak (1971) *Proc Inter Conf Physics Semiconductors*, Institute of Physics and physical society, London; *Phil Mag* 22: 519.
 40. X Ledecac (1979) *J Physique* 40: 27.
 41. K Shimakawa (1978) *Phil Mag* 46: 123.
 42. M Pollak and GE Pike (1972) ac Conductivity of Glasses. *Phys Rev Lett* 28: 1449.
 43. LG Austin and NF Mott (1969) Polarons in crystalline and non-crystalline materials. *Adv Phys* 18: 41-102.
 44. CA Hogarth, MH Islam and ASMS Rahman (1993) D.c. and a.c. electrical properties of vacuum evaporated thin SiO/GeO_2 films. *J Materials Science* 28: 518-528.
 45. CGB Garrett (1960) *Mater Des Eng* 51: 12.
 46. F Gutmann and LE Lyons (1967) "Organic Semiconductors". Wiley, New York 1967: 5.
 47. DD Eley (1948) Phthalocyanines as Semiconductors. *Nature* 162: 819.
 48. DD Eley, GD Parfitt, MJ Perry and DH Taysum (1953) The semiconductivity of organic substances. Part 1. *Trans Faraday Soc* 49: 79.
 49. DD Eley and GD Parfitt (1955) The semiconductivity of organic substances. Part 2. *Trans Faraday Soc* 51: 1529.
 50. H Hansel (1970) Diffusion of metals in metals. *Ann Phys* 24: 1947.
 51. DC Olson, VP Mayweg and GN Schrauzer (1966) Polarographic Study of Coordination Compounds with Delocalized Ground States. Substituent Effects in Bis- and Tris(dithiodiketone Complexes of Transition Metals. *J Am Chem Soc* 88: 4874-482.
 52. F Gutmann and A Netschey (1962) Electrical Properties of Chlorpromazine. *J Chem Phys* 36: 2355.
 53. F Gutmann and H Keyzer (1965) Electrical Conduction in Chlorpromazine. *Nature* 205: 1102-1103.
 54. MS Hossain, R Islam and KA Khan (2008) Electrical conduction mechanisms of undoped and Vanadium doped ZnTe thin. *Chalcogenide Letters* 5: 1.
 55. AH Pohl (1964) Physico-chemical aspects of organic semiconductors. *Prog Solid State Chem* 1: 316.
 56. JJ Brophy and WJ Buttrey (1962) Organic Semiconductors. Proceeding of an Inter-Industry Conference, Macmillan.
 57. SS Haggag, MM Syiam, HM Klash, II Mahmoud (2004) Hardware implementation of neural network on FPGA for accidents diagnosis of the multi-purpose research reactor of Egypt. *IEEE* 43: 77.
 58. AA Shabana, KA El-Manakhly and HA Hammad (1994) *Can J Appl Spectrosc* 39: 151.
 59. BA El-Sayed, MM El-Desoky, SM Shaaban and MB Sayed (1990) Electrical and spectral studies of solid organic semiconductors I. Structural interpretation of promoted conductivity of salicylaldazine. *Electrochim Acta* 35: 1987.
 60. MS Masoud, ME Kassem, Y Abd El-Aziz and SM Khalil (1991) Electrical conductivity of some azo complexes containing sulphur. *Bull Fac Sci, Mansoura University* 18: 105-118.
 61. MS Masoud, EA Khalil, EEI-Shereafy and SA Abou El-Enin (1990) Thermal and electrical behaviour of nickel (II) and copper (II) complexes of 4-acetamidophenylazo-p-cresol (4-acetylamino-2-hydroxy-5-methyl azobenzene) *J Therm Anal* 36: 1033-1036.
 62. MS Masoud, ZM Zaki, FM Ismail and AK Mohamed (1997) Electrical conductivity behaviour of 5-substituted arylazothioibarbituric acid complexes at different temperatures. *Z Phys Chem, Bd* 185: 223-231.
 63. MS Masoud, ZM Zaki and FM Ismail (1989) Conducting Properties of Some New Azo-Nitroso Complexes. *Thermochim Acta* 156: 225-230.
 64. AAG Tomlinson and BJ Hathaway (1968) The Electronic Properties and Stereochemistry of the Copper(II) Ion. Part III. Some Penta-ammine Complexes. *J Chem Soc A* 1968: 1905-1909.
 65. E El-Shereafy, SA Abou El-Enin, M Khider and H El-Esawy (2004) *Bull Fac Sci Alex Univ* 43: 67.

-
66. S Chen, JF Richardson and RM Buchanan (1994) Synthesis and Characterization of Copper(II) Complexes of New Tripodal Polyimidazole Ligands. *Inorg Chem* 33: 2376-2382.
 67. Y Dong, H Fujii, MP Hendrich, RA Leising, G Pan, et al. (1995) A High-Valent Nonheme Iron Intermediate. Structure and Properties of $[\text{Fe}_2(\mu\text{-O})_2(5\text{-Me-TPA})_2](\text{ClO}_4)_3$. *J Am Chem Soc* 117: 2778-2792.
 68. RG Pearson (1986) Absolute electronegativity and hardness correlated with molecular orbital theory. *Proc Natl Acad Sci* 83: 8440-8441.
 69. T Koopmans (1934) Über die Zuordnung von Wellenfunktionen und Eigenwerten zu den Einzelnen Elektronen Eines Atoms. *Physica* 1: 104-113.
 70. RG Parr, RA Donnelly, M Levy and WE Palke (1978) Electronegativity: The density functional viewpoint. *J Chem Phys* 68: 3801.
 71. RG Parr and RG Pearson (1983) Absolute hardness: companion parameter to absolute electronegativity. *J Am Chem Soc* 105: 7512-7516.
 72. EM Zueva, VI Galkin, AR Cherkasov and RA Cherkasov (2002) Electronic Chemical Potential and Orbital Electronegativity of Univalent Substituents. *Russian J Org Chem* 38: 624-631.
 73. RG Parr, LV Szentpály and S Liu (1999) Electrophilicity Index. *J Am Chem Soc* 121: 1922-1924.
 74. PK Chattaraj, U Sarkar and DR Roy (2006) Electrophilicity Index. *Chem Rev* 106: 2065-2091.
 75. PK Chattaraj and DR Roy (2007) Update 1 of: Electrophilicity Index *Chem Rev* 107: 46-47.

Copyright: ©2021 MS Masoud, et al. This is an open-access article distributed under the terms of the Creative Commons Attribution License, which permits unrestricted use, distribution, and reproduction in any medium, provided the original author and source are credited.